LAWRENCE
LIVERMORE
NATIONAL
LABORATORY

LLNL-TR-409526

LIFE Materails: Molten-Salt Fuels Volume 8

R.W. Moir, N. Brown, A. Caro, J.C. Farmer, W. Halsey, L. Kaufman, K. Kramer, J. Latkowski, J. Powers, H. Shaw, P.E.A. Turchi

December 19, 2008

Disclaimer

This work performed under the auspices of the U.S. Department of Energy by Lawrence Livermore National Laboratory under Contract DE-AC52-07NA27344.

Molten-Salt Fuels

Volume 8

R. W. Moir, R. Abbott, N. Brown, A. Caro, J. C. Farmer, W. Halsey, L. Kaufman, K. Kramer, J. Latkowski, J. Powers, H. Shaw, P. E. A. Turchi

Physical and Life Sciences Directorate

National Ignition Facility and Photon Sciences Directorate

Lawrence Livermore National Laboratory

7000 East Avenue

Livermore, California 94550

July 15th 2008 —First Draft

November 20th 2008—Revision n

December 1st 2008—Revision n+1

Executive Summary

The goals of the Laser Inertial Fusion Fission Energy (LIFE) is to use fusion neutrons to fission materials with no enrichment and minimum processing and have greatly reduced wastes that are not of interest to making weapons. Fusion yields expected to be achieved in NIF a few times per day are called for with a high reliable shot rate of about 15 per second. We have found that the version of LIFE using TRISO fuel discussed in other volumes of this series can be modified by replacing the molten-flibe-cooled TRISO fuel zone with a molten salt in which the same actinides present in the TRISO particles are dissolved in the molten salt. Molten salts have the advantage that they are not subject to radiation damage, and hence overcome the radiation damage effects that may limit the lifetime of solid fuels such as TRISO-containing pebbles. This molten salt is pumped through the LIFE blanket, out to a heat exchanger and back into the blanket. To mitigate corrosion, steel structures in contact with the molten salt would be plated with tungsten or nickel. The salt will be processed during operation to remove certain fission products (volatile and noble and semi-noble fission products), impurities and corrosion products. In this way neutron absorbers (fission products) are removed and neutronics performance of the molten salt is somewhat better than that of the TRISO fuel case owing to the reduced parasitic absorption. In addition, the production of Pu and rare-earth elements (REE) causes these elements to build up in the salt, and leads to a requirement for a process to remove the REE during operation to insure that the solubility of a mixed (Pu,REE)F3 solid solution is not exceeded anywhere in the molten salt system. Removal of the REE will further enhance the neutronics performance. With molten salt fuels, the plant would need to be safeguarded because materials of interest for weapons are produced and could potentially be removed.

The report is Volume 8 of a set of 12 volumes on aspects of LIFE:

1. • Volume 1 – Overview of Fuels & Structural Materials Issues
2. • Volume 2 – Design & Fabricability
3. • Volume 3 – Transmutation & Phase Formation
4. • Volume 4 – Radiation Effects
5. • Volume 5 – Thermomechanical Effects
6. • Volume 6 – Corrosion & Environmental Cracking
7. • Volume 7 – Molten-Salt Coolants
8. • Volume 8 – Molten-Salt Fuels
9. • Volume 9 – On-Site Solid-State Tritium Storage

10. • Volume 10 – Proliferation Resistance
11. • Volume 11 – Fuel Cycle & Repository
12. • Volume 12 – Licensability
13. • Volume 13 – Cost mode

14. Table of Contents

List of Tables

List of Figures

Chapter A. LIFE Requirements for Molten-Salt Fuels

As an alternative to the TRISO and other solid fuel versions of LIFE, we are assessing the feasibility of developing a LIFE engine that has a fission blanket consisting of a molten salt into which fertile or fissile fuel is dissolved. If it is not possible to develop a solid fuel form that can withstand the effects of the cumulative radiation damage suffered at the burnups desired for the LIFE mission, which are typically considered to be >0.95 Fissions per Initial heavy Metal Atom, (FIMA, commonly written as a percentage, e.g., >95% FIMA), then molten salt fuels offer a path forward because they do not suffer radiation damage. A disadvantage of molten salts is that they must undergo some amount of processing during the operation of the engine. This could provide an opportunity to access fissile material, and hence leads to proliferation concerns that can be addressed by appropriate safeguards. If the solid fuels capable of achieve lifetimes consistent with high burnup cannot be developed, then the solid fuel will also need to undergo processing for further burning, so this relative disadvantage would disappear. There is also a need to give further consideration to the safety of the molten-salt fuel. Two barriers to fission product release that are present in the solid fuel have been removed in the molten-salt. The solid fuel form retains fission products, even some noble gas, within its structure. However, this may no longer be true at the very high burnup especially when the gaseous fission products have built up to high pressure. The solid fuel is also coated or imbedded in a fission product retaining structure that is not present in the molten-salt. These two barriers are important factors in the safety assessments conducted on the current generation of reactors. In the case of molten salt fuel the gaseous fission products are continuously removed and the other fission products are contained in the melt. The primary loop is a containment boundary; the room is lined with a fission product barrier including drain tanks to receiving spilled molten salt in case of a breach. The last boundary is the confinement building.

We assume the fusion systems (laser, target, fusion power, tritium system, chamber clearing), as well as the first wall, are the same as for the main solid fuel case and will not discuss them here.

To date, most of the calculations of the neutronic performance of LIFE engines have involved solid fuel pebbles containing TRISO particles. Calculations for the molten salt fuel case indicate that the nuclear performance of the molten salt fuel is similar enough to the TRISO fuel case that we only discuss the differences between these cases.

History of molten salts used in reactors

A molten salt reactor (MSR) is a type of nuclear reactor in which the nuclear fuel is dissolved in a molten salt, which also acts as the primary coolant. There have been many designs put forward for use of this type of reactor to generate electricity or hydrogen, produce fissile material (breed), or fission transuranic actinides, and a few prototypes have been built. The concept is also one of six reactor types proposed for development as a Generation IV (Gen-IV) reactor. The initial reference design for the Gen-IV MSR (Fig. 1) would be 1000 MWe with a deployment target date of 2025.

Extensive research into molten salt reactors started with the US **Aircraft Reactor Experiment** (ARE). The US Aircraft Reactor Experiment was a 2.5 MW_{th} nuclear reactor experiment designed to attain a high power density for use as an engine in a nuclear powered bomber. The project resulted in several experiments, three of which resulted in engine tests collectively called the Heat Transfer Reactor Experiments: HTRE-l, HTRE-2, and HTRE-3. One experiment used the molten fluoride salt NaF-ZrF_4-UF_4 (53-41-6 mol%) as fuel, was moderated by beryllium oxide (BeO), used liquid sodium as a secondary coolant, and had a peak temperature of 860 °C. It operated for a 1000-hour cycle in 1954. This experiment used Inconel 600 alloy for the metal structure and piping.

Oak Ridge National Laboratory took the lead in researching the MSR through the 1960s, and much of their work culminated with the Molten-Salt Reactor Experiment (MSRE). The MSRE was a 7.4 MW_{th} test reactor simulating the neutronics "kernel" of an inherently safe epithermal thorium-breeder reactor. It tested molten salt fuels of uranium and plutonium. The 650 °C temperature of the reactor could power high-efficiency heat engines such as gas turbines. The large, expensive breeding blanket of thorium salt was omitted and the space used for neutron measurements.

The MSRE was located at ORNL. Its piping, core vat and structural components (Figure 2) were made from Hastelloy-N and its moderator was pyrolytic graphite. It went critical in 1965 and ran for four years. The fuel for the MSRE was LiF-BeF_2-ZrF_4-UF_6 (65-30-5-0.1), the graphite core moderated it, and its secondary coolant was flibe (2LiF-BeF_2). It reached temperatures as high as 650 °C and operated for the equivalent of about 1.5 years of full power operation. In 1976, work on the molten salt reactor in the U.S. ended, and the country's reactor program focused on the development of just one breeder reactor concept, the metallic sodium-cooled fast reactor. Nevertheless, the MSRE stands as a demonstration of the viability of the concept, and our assessment of the feasibility of a molten-salt-fueled LIFE engine is largely based on the data and experience gained from work on the MSRE.

Related work on molten salt fuel from Gen-IV fission reactor program

The inclusion of a MSR concept as one of the Generation-IV (Gen-IV) reactor designs has stirred renewed interest in this technology. This international effort should generate much relevant R&D useful for LIFE studies, particularly in the areas of molten salt physical chemistry and thermodynamics, on-line salt processing and waste handling, and the development of compatible structural materials. The major Gen-IV effort is directed towards closing the fuel cycle, with an emphasis on economic sustainability, safety, and proliferation resistance. (Technology Roadmap, 2002)

Goals for Generation IV Nuclear Energy Systems

Sustainability–1 Generation IV nuclear energy systems will provide sustainable energy generation that meets clean air objectives and promotes long-term availability of systems and effective fuel utilization for worldwide energy production.

Sustainability–2 Generation IV nuclear energy systems will minimize and manage their nuclear waste and notably reduce the long-term stewardship burden, thereby improving protection for the public health and the environment.

Economics–1 Generation IV nuclear energy systems will have a clear life-cycle cost advantage over other energy sources.

Economics–2 Generation IV nuclear energy systems will have a level of financial risk comparable to other energy projects.

Safety and Reliability–1 Generation IV nuclear energy systems operations will excel in safety and reliability.

Safety and Reliability–2 Generation IV nuclear energy systems will have a very low likelihood and degree of reactor core damage.

Safety and Reliability–3 Generation IV nuclear energy systems will eliminate the need for offsite emergency response.

Proliferation Resistance and Physical Protection–1 Generation IV nuclear energy systems will increase the assurance that they are a very unattractive and the least desirable route for diversion or theft of weapons-usable materials, and provide increased physical protection against acts of terrorism.

The Gen-IV report (A Technology Roadmap, 2002,pp. 33 - 37) summarizes the molten salt option and suggests $1000M of R&D funding for a 16 year period (2004 to 2030) broken down into the following areas: Materials-(200 M$); Reactor Systems (150 M$); Balance of Plant (50 M$); Safety (200 M$); Design & Evaluation (100 M$); Fuel Cycle (300 M$).

Four possible missions for LIFE engines

With the same fusion neutron source the fission blanket of a LIFE engine can be designed for different missions. The following are four such possible missions for a LIFE program to consider.

1. **The power mode with its own wastes burned**. ^{238}U (depleted uranium) and/or ^{232}Th dissolved in molten salt and burned to completion (FIMA----->100%).

2. **The power mode with spent nuclear fuel burned**. Remove Zircaloy cladding from spent fuel, reduce the oxides, convert to fluorides and dissolve in molten salt and burn to completion (FIMA----->100%).

3. **The Pu and minor actinides burner.** Remove the uranium from spent fuel, and burn to completion the Pu and minor actinides (FIMA----->100%). Alternatively, the Pu could be separated and burned in fission reactors leaving only the minor actinides to burn in LIFE engines. The feedstock could be weapons Pu.

4. **The fuel factory mode.** ^{232}Th dissolved in molten salt; remove ^{233}U for use in fission client reactors (^{232}U/^{233}U>>2.4% for non-proliferation[1]) fission is suppressed, FIMA<<100%.

Preliminary studies indicate that it will be necessary to keep the sum of the concentrations of the trivalent actinides and lanthanides below approximately 1 mole percent of the total cations in order to maintain solubility. This would suggest reducing the amount of U in the melt because it produces Pu by neutron capture. Furthermore, fission of both U and Pu produces substantial amounts of lanthanides. We could start with a small amount of UF_4 for example 2 mol% and ThF_4 22 mol%. This would be appropriate if we removed the uranium in spent fuel and feed the Pu and minor actinides to LIFE for burning. The Pu production would be greatly reduced, and one could add Pu just as it is burned to keep it below the solubility limit. Processing to remove the REE would still be required, however.

---

1. The dose rate at 1 meter from 5 kg of ^{233}U one year after chemical separation is 100 rem/hr or 1 Sv/hr for $^{232}U/^{233}U$ =2.4%.

Chapter B. Summary of Existing Knowledge

As a starting point we can consider a study of a tandem mirror fusion fission fuel breeder because it used molten salt fuel (Lee et al., 1982). Chapter IV of this report has 98 pages discussing the molten salt blanket mechanical design, with other parts of the report discussing fuel cycles and other aspects.

Liquid lithium was used as the neutron multiplier and the fuel-breeding zone used molten salt as shown in Figure 3. Being liquids, neither the lithium neutron multiplier nor the fuel zone are subject to radiation damage. The structural material was 316 SS. To limit corrosion a frozen salt layer in the molten salt region was employed. The molten salt was processed by fluorination to remove fissile material that was kept to such a low concentration so as to suppress fission. The fissile production rate is about 0.49 atoms per fusion neutron. The ^{233}U produced was at a rate of 1060 kg/y for 500 MW of fusion power. The ^{232}U produced along with the ^{233}U (~0.2% $^{232}U/^{233}U$) gives a strong gamma ray emission such that the fuel is proliferation resistant in that the material is not desirable as a military weapon and detection is made easier, although it could make a terrorist weapon where those near by attending the weapon would receive a considerable dose of radiation.

For the LIFE application we can modify this design. The first wall and beryllium neutron multiplier of LIFE can be used instead of the lithium multiplier in order to produce more neutrons, however, radiation damage will limit the beryllium lifetime. The 80-cm zone of molten salt as shown above can be retained, that is, the flibe-cooled region of pebbles containing TRISO fuel particles in LIFE can be replaced with this molten salt zone. The molten salt containing actinide fuel must be separate from the flibe loop cooling the beryllium because otherwise the beryllium would reduce the fuel salt. A break between the two salt loops represents another failure mode. The 316 SS can be replaced with 304 SS with close to the same corrosion properties and much less production of long-lived neutron activation products of Nb and Mo, both of which are not called for in the 304 SS alloy.

The idea of using SS rather than the nickel alloy, Hastelloy[2] is that nickel radiation damages fairly rapidly. The corrosion resistance is obtained from the nickel in stainless steel. The corrosion leaches or dissolves out Cr (and to a lesser extent, Fe) near the surface, leaving a nickel-enriched surface, making in effect a nickel coating. However, LIFE studies have chosen ferritic steel for its first wall and structures. For corrosion resistance we might chose to coat the

2. Hastelloy-N is a nickel alloy of the following approximate constituents in wt%: Ni 80, Mo 12, Cr 7, Nb 1.

steel with nickel or tungsten. The piping and structures outside the neutron environment would use Hastelloy.

The adaptation blanket for LIFE is shown in figure 4 below. The thickness shown here at 80 cm has not been optimized. A mixture of Th and U is shown with a graphite reflector.

Cheng, 2003 and Cipita et al., 2006 have carried out a series of studies for tokamak fusion systems for burning actinides in molten salt.

LIFE mechanical design summary

The mechanical design and layout of a liquid fueled LIFE chamber will inherit heavily from the solid-fueled option (Abbott, 2009). This is natural as both systems face many common requirements. The geometry will still need to allow for central hot-spot ignition. The first wall will still require dedicated cooling to remove conducted fusion ion and x-ray energy. The beryllium multiplier will still need to be in pebble form so that removal and swelling treatment can be performed. For the molten-salt-fueled engine, the plenum holding the Be multiplier pebbles will need to be isolated from the fuel region to avoid reduction of the dissolved actinides by the Be metal. The Be wall separating these regions multiplier region will therefore need a separate system for circulating flibe (or other coolant).

Figure 5 shows a cross-section looking down on the current solid-fuel LIFE chamber showing dedicated first wall cooling with a lithium lead eutectic (purple) as well as primary coolant (blue) injection and extraction manifolds. For an in depth discussion of the details of this chamber design see Reference (Abbott, 2009).

The only significant geometric change that will be required is the removal of the partition separating the solid fuel (red) region from the reflector (grey) region. In the molten salt-fueled design these two regions would become a single region filled with graphite pebbles at 70% packing for moderation. To achieve such a high packing fraction will likely require multiple pebble sizes or non-spherical pebble geometry.

The molten salt that served as the coolant in the solid-fuel chamber would now contain the fuel, but this fluid would still serve to remove thermal energy from the various solid structures as it travels radially outward toward the extraction plenum. Detailed thermal-hydraulics calculations for this liquid-fueled design have not yet been completed but given equivalent power densities to the solid fuel case, flow rates, pressure drops, structural loads, and static stresses should be comparable. Dynamic pressure pulsing from isochoric heating of molten salt will likely be larger, because the fission thermal energy is directly deposited in the liquid fuel option.

Structural material with a higher operational temperature window than 12YWT used for the solid-fuel chamber will be required for the liquid fuel chamber. The fuel-salt composition has a melting temperature well above that for the pure flibe being used in the solid fuel chamber and an ODS ferritic steel able to maintain its strength in the 700 to 750 °C range will be required.

Temperature distribution in the primary loop of LIFE with molten salt fuel

Thermal hydraulic designs and calculations for the design are needed. Initial estimates for temperatures at key points are given above. The melt temperature comes from the phase diagrams dealing with solubility of PuF_3. T_{melt}=610 °C comes from this analysis. The coldest part of the heat exchanger needs to be safely above the melt temperature. Assuming a safety margin of 30 °C means that in the coldest portion of the loop, T_{cold}=640 °C. Assuming a 30 °C drop across the film of turbulent flowing molten salt then the inlet temperature to the molten salt blanket is T_{in}=670 °C. Assuming the molten salt in the blanket heats up by 50 °C then the blanket outlet temperature is T_{out}=720 °C. If the hottest part of the blanket is cooled by the exiting molten salt with the same 30 °C as assumed before, then the structural hot spot is $T_{structural\ hot\ spot}$ =750 °C. If the hottest part of the structure is cooled with other than exiting flibe then $T_{structural\ hot\ spot}$ = T_{out}= 720 °C. The important temperatures are constrained by solubility considerations on the low end of T_{melt}≈610 °C and by structural temperatures limits on the high end of $T_{structural\ hot\ spot}$ = 720 to 750 °C.

Structural materials

The radiation damage considerations for the steel used for molten salt version of LIFE is very similar to the version using TRISO fuel. Therefore we refer the reader to the TRISO fuel, structural materials reports for discussion of this topic. However, corrosion is specific to the molten salt fuel design and the higher temperature will require different ferritic material.

The molten salt containing UF_4 is aggressive towards corrosion of structural materials. Our choices are:

1. use a frozen salt layer on the structural material to slow corrosion
2. use stainless steel (304) and allow leaching to enrich nickel on the surface to look like Hastelloy
3. coat steel with Mo, W or Ni to inhibit corrosion.

We cannot use the frozen layer approach to corrosion inhibition because of the potential for accumulation of solids containing fissile materials (e.g., Pu) in the layer, with attendant criticality concerns. We cannot use 300-series stainless steel because the thermal conductivity is two to three times lower than for ferritic steel, an important parameter in thermal stress and the radiation damage is more severe in 300 austenitic than in ferritic steel. This leaves us with using coatings for corrosion resistance. Tungsten is assumed for the first wall and could be used to coat the structural components that face the molten salt; however, Ni is easier to coat and will be adequate for molten salt corrosion resistance. Furthermore it is much cheaper than W. A study

of the coating of steel with W as armor for the first wall seems to show no problem with regard to fatigue at the interface. Fe and W form stable intermetallics and the bonding is very good (Blanchard and Martin, 2005). Ni forms weaker compounds and the cohesion of the interface under the thermal cycle has to be considered. Therefore the choice of coating material needs further study.

Conversion of material to form suitable for molten salt

We assume the fuel feedstock material is either in metallic or oxide form and would need to be converted to fluoride form and added to the molten salt. The feedstock might be depleted uranium, or spent nuclear fuel in oxide form. A simplified flow sheet for the processes of converting spent nuclear fuel to a form useable in a molten salt LIFE is given in Figure 7. For more discussion on the options for burning LWR SNF in LIFE Engine see ref (Farmer et al., 2008).

Spent fuel–oxide form

The oxide can be converted by hydro-fluorination at temperatures of 825 to 875 K (Eykens, Pauwells and Van Adenhove, 1985):

$UO_2 + 4HF + 1/2H_2 \rightarrow UF_4 + 2H_2O + 1/2H_2$

$PuO_2 + 3HF + 0.5H_2 \rightarrow PuF_3 + 2H_2O$

The resulting fluorides are in granular form and can be added to the molten salt as discussed below. If it is desired to burn only the Pu and minor actinides, then the uranium could be removed by producing volatile uranium hexafluoride in a further fluorination step:

$UF_4 + F_2 \rightarrow UF_6$

The fluorine potential would need to be controlled to avoid the production of volatile PuF_6; alternatively, any PuF_6 produced could be recovered by thermal decomposition to $PuF_4 + F_2$.

Pu–metallic form

We assume a feedstock of metallic Pu in the form of metal parts or oxides. This would be appropriate to the weapons Pu mission and is discussed in a separate report. PuO_2 feedstock can be converted to trifluoride *via* the hydro-fluorination reaction given above. For metallic Pu, suitably small pieces of metal would be fed into a furnace for hydriding.

$Pu + H_2 + He \rightarrow PuH_2 + He$ at 100 to 200 °C

The PuH_2 is in a powdery form. The next step is a conversion to fluoride at < 100 °C in a nickel chamber. Helium aids removal of the heat from the exothermic reaction:

PuH_3 +3HF+ He--->PuF_3+3/2H_2+ He

The PuF_3 is in the form of fine grains. The foregoing is based on discussions with R. Condit, 2008.

The above process steps would likely be a combination of batch and continuous processes. Care would be needed to ensure criticality safety at all times under all conditions.

The granular UF_4+PuF_3 + other actinides can be augured slowly into a flowing molten flibe salt and allowed to dissolve. Another, possibly preferred, alternative would be to add solid BeF_2 and LiF salts to the PuF_3, then melt this mixture and add the melt to the flowing molten salt.

Control of redox potential of salt

We must make sure the solubility of Pu, other actinides, and fission products in the molten salt is not exceeded as they build up during the burn. The solubility is temperature dependent. The molten salt will be continuously pumped to a heat exchanger and back to the blanket. A small side stream will be processed to remove certain elements produced by the fission process and impurities, and to "doctor" the salt. The average oxidation state of the fission products produced during the burn is less than +3, considerably lower than the +4 the initial oxidation state of most of the uranium fuel. The redox potential (strictly speaking, the fluoride potential) of the molten salt will therefore need to be controlled during the burn by continuously adjusting the ratio of UF_4/UF_3 to lie in the range of ~20 to 40. As the concentration of U in the salt decreases during the burn, its effectiveness as a redox buffer will be reduced, and at some point, its concentration will be so low that the U^{3+}/U^{4+} couple no longer has sufficient buffer capacity to control the redox state of the salt. It will therefore be necessary to identify another redox couple that can buffer the redox state of the salt at high burn-up. The redox couple, Ce^{3+}/Ce^{4+} has been used in laboratory work in the past; however, maintaining the redox state of the salt at a level low enough to prevent corrosion of structural metals requires a very high Ce^{3+}/Ce^{4+} activity ratio (Olander, 2002).

The tritium that is formed by neutron reaction with lithium should quickly react homogeneously, that is, in the bulk, to become TF. The TF itself should quickly react according to the reaction:

UF_3+TF----->1/2T_2 + UF_4

Thus, the production of TF will consume UF_3 in the melt, leading to a requirement for a means to maintain the U^{3+}/U^{4+} within the desired bounds. The on-line salt processing system (see below) will therefore need to be designed to accommodate this requirement.

If the TF "sees" a Fe atom or a Cr atom before it sees a UF_3 molecule it will react to form FeF_3 or CrF_3, that is, corrosion will take place. This reaction is slow because it only occurs at a surface, that is, heterogeneously. Nickel is stable in the presence of TF so it does not corrode (no reaction). The corrosion rate of steel then becomes a rate question.

Neutronic performance

Peter Song, 2008, performed preliminary studies of molten salt candidates for LIFE and more extensive studies were carried out by Jeff Powers, 2008. The results of those studies are summarized here. The starting composition of the molten salt was: LiF (76 mol%) + UF_4 (12 mol%) + ThF_4 (12 mol%). The mixture of U and Th was used to lower the peak concentration of Pu in the salt. With a steady 500 MW of fusion power the total thermal power was kept at 2000 MW by adjusting the ^6Li to ^7Li ratio over time. Graphite was added as a moderator. The optimum fuel-to-moderator ratio found in the Powers study was 70 vol% graphite and 30 vol% molten salt. It should be noted that in the burn calculations, the moderator was included via volumetric homogenization of molten salt and graphite due to modeling limitations.

For these calculations, it was assumed that the noble gas fission products were removed from the salt on a rapid timescale by sparging of the melt with He gas (Engel et al, 1980). Furthermore, the noble and semi-noble metal fission products do not form soluble fluoride complexes at the fluoride potential of the melt and are insoluble. The elements in this category include: Zn, Ga, Ge, As, Nb, Mo, Tc, Ru, Rh, Pd, Ag, Cd, In, Sn, and Sb. Experience with the ORNL Molten Salt Reactor Experiment (MSRE) (Compere et al., 1975) suggests that these elements form multi-atom metallic clusters in the melt. In the MSRE, some of these elements were removed as particulates in the sparge gas, some plated out on the metal walls of blanket structures and piping and heat exchangers, and the remaining fraction circulated in the molten salt. As discussed in the section on processing, below, some form of on-line processing will be needed to actively remove these elements from the melt. The burn calculations therefore assumed that these elements were removed from the salt as soon as they were produced.

The results of a partially optimized molten salt burn calculation are compared with a base-case solid-fuel calculation in Figure 7. As Pu and ^{233}U build up, the fission power rapidly rises to the total desired power of 2000 MW and is held at this level for approximately 60 years. Then, as the tritium inventory is exhausted, the power declines until a burnup of 99% FIMA is reached. The burn curve was improved due to the additional $^6Li(n,t)\alpha$ tritium production in the molten salt from thermal and epithermal neutrons. As expected the performance is somewhat better than for the TRISO fuel case (da0) owing to the removal of the noble gas and noble/semi-noble metal fission products.

The evolution of the composition of the molten salt for this case is shown in Figure 9. The Pu concentration peaked at 2.2 mol%, and the concentration of all the transuranic elements

(Pu+Np+Am+Cm) is only slightly larger than Pu alone. This plot also shows the real issue, namely that the sum of the trivalent actinides and rare-earth elements (REE) would approach 10 mol% in the salt. These elements essentially behave as a single element in molten fluoride salts, and form a mixed actinide+REE trifluoride solid solution. The solubility of this phase, as we discuss below, is only on the order of 1-3 mole % in low-BeF_2 compositions. A salt composition containing 10 mol% trivalent actinides and REE would therefore precipitate this solid trifluoride. We therefore need to keep the dashed line decorated with solid triangles in Figure 9 below the appropriate solubility (i.e., the solubility at the minimum temperature of the low-temperature loop). This will require removal of the REE during operation. Going to a Th fuel cycle will not help the REE solubility problem because the high-mass peak of the fission yield curve for ^{233}U still lies in the region of the light REE; however, no Pu is made.

The production of ^{232}U and ^{233}U from ^{233}Th is shown in Figure 10. During the burn we build up a peak total fissile inventory of ^{233}U + Pu of about 2 metric tonnes. The U is self protected somewhat by the buildup of ^{232}U as is shown by Figure 11.

Another set of neutronics calculations was performed assuming removal of REE as well as the noble gases and noble/semi-noble metals, and, as expected, the performance was a somewhat better, but similar to that shown in Figures 8-11. The evolution of the composition of the salt for this burn case is shown in Figure 12. The Pu peaked at 2.3 mol% and the sum of Pu+Np+Am+Cm peaked at 2.5%. The fission products Ba, Zr, Cs, Te, Y, Sr were not removed for the purposes of this calculation.

In order to reduce the peak PuF_3, a case was run for 6 mol% UF_4 and 18 mol% ThF_4 and the peak Pu concentration dropped to 1.2 mol%.

To use LIFE in a breeder mode, one would process fissile material before it is allowed to build up and fission, thereby suppressing fission. Preliminary calculations (Song, 2008) found a breeding ratio of about 0.6 at the beginning of life of LIFE engine; that is, 0.6 fissile atoms are produced for each fusion neutron produced. This amounts to about 1000 kg of Pu per 500 MW_{fusion}· year. In the case of fertile, Th-only blanket, the fissile product would be ^{233}U, which would be separated from the molten salt by fluorination. The ^{232}U that is also produced would self-protect this material somewhat reducing proliferation concerns; however, the facility would need to be safeguarded. In this case, the ^{232}U fraction of the product will be far higher than that shown in Figure 11 owing to the buildup of ^{231}Pa and lower concentration of ^{233}U; however, a calculation has not yet been done for this case. In another related configuration without a beryllium multiplier the $^{232}U/^{233}U$ ratio was well over 10% in the fissile product. With $^{232}U/^{233}U$ =10% the dose rate at 1 m from 5 kg of bare ^{233}U one year after separation is 420

rem/hr or 4.2 Sv/hr, which is over 4 times higher than the IAEA's standard for reduced physical protection requirements (>100 rem/hr at 1 meter) (International Atomic Enery Agency).

Although these initial findings are very encouraging, more work is required to optimize the design. For instance, additional studies of $LiF/UF_4/ThF_4$ molar ratios will be performed to determine if the mole fraction of Pu and rare earth elements can be kept below a 1-3 mol% solubility limit. If not, the lowest limit attainable will be ascertained.

Our current analysis tools limit the scope of scenarios that we can examine; however, additional software development will allow for variable input streams of $LiF/UF_4/ThF_4$ over time to potentially prevent excessive build up of Pu and REE. Likewise, the solubility concerns could be addressed through clever alteration of fuel-to-moderator ratios at different points in the burn cycle. These code enhancements will allow for additional design scoping and analysis.

Analysis of criticality safety during off-normal operation has only just begun. Although the molten salt blanket is designed to be subcritical at all times during normal operation, further analysis is required to assure the fuel stays subcritical in all possible accident scenarios.

The following are issues that need further examination.

Zr has a low melting point (sublimation) and is likely to have a fairly high vapor pressure as ZrF_4. This might allow removal by distillation, though reductive extraction into a molten metal (e.g., Bi) containing an alkali reductant would also be effective (see processing discussion below). In future studies we can get vapor pressure data. The low melting point of ZrF_4 should lower the eutectic temperature of the salt, and should increase Pu solubility at a given temperature.

Melting temperatures of NpF_3, AmF_3, and CmF_3 are needed; however, their concentrations are so much lower than Pu that these data are probably not of great importance.

Tm, Yb, and As are not in the neutronics calculation data base and hence some small errors may have resulted.

BaF_2, SrF_2 and YF_3 have high melting points and high concentrations. Y, which has chemistry similar to the intermediate-mass REE, should be removed in any on-line processing system designed to remove the REE. Ba and Sr removal may be possible, but does not appear to be necessary from a neutronics or solubility standpoint.

Molten salt composition

Among the several competing properties that have to be considered in choosing a salt, the nuclear and chemical properties are arguable the most important. The neutronic constraint is measured by the neutron capture probability by the salt constituents. Firstly, a large capture

cross-section leads to a loss of neutrons, so elements with the smallest cross-sections are preferred. Secondly, the production of new isotopes may be undesirable because they may have unacceptably large neutron cross-sections, because they have undesirable chemistry (e.g., they form low-solubility solids, or are corrosive to structural materials), or because they are long-lived nuclides of concern from a disposal standpoint. Table 3 gives a ranking of the nuclear properties for candidate salt constituents, thus constraining candidate salt selection on the basis of chemical constraints (Williams, Toth and Clarno, 2006).

As far as the salt chemistry is concerned, the main requirement (besides an acceptable viscosity and favorable nuclear properties) is its stability (to prevent problems during the circulation of the salt caused by precipitation). The precipitation of solids may occur during cooling, and also over time (*i.e.*, as a function of burn-up) from the build-up of fission products and actinides produced by nuclear reactions, corrosion of structural materials, or by accidental contamination (e.g., by water vapor). Hence there is a need for online processing to control the chemistry of the salt. These chemical constraints necessitate an accurate knowledge of fuel thermochemistry and phase diagrams for the purpose of not only selecting an optimal molten salt fuel composition, but also for subsequent on-line chemical processing of the fuel during the entire operational life of the LIFE engine.

The neutronic constraint has led over the years to the selection of a class of salts, namely the fluorides (N.B.: since this study is still at an early stage, the chloride option that has been less studied will not be considered in the report, although better solubility for Pu and other actinides can be achieved when using a matrix based on alkali metal halides). As part of the requirements, to be an acceptable candidate, a molten salt should:

- be thermally stable over the operating temperature range;
- be resistant to radiation;
- provide adequate solubility for U, Th, and other actinides at temperatures safely below the temperature at which the fuel will operate;
- have a small neutron capture cross-section;
- have a low vapor pressure (for safety reasons);
- exhibit no or minimal reaction with the Ni-based alloy cladding of the containment vessel;
- be capable of an economical online processing scheme;
- be inexpensive to make the whole option economically viable.

Additional constraints have to be considered such as: melting temperature, viscosity, and heat capacity. Among the most promising salts that are currently considered for fast breeder reactors, the following are worth mentioning:

- ^{7}LiF-BeF_2 mixture for optimum breeding conditions;
- ^{7}LiF-NaF mixture for optimum spectrum; and
- ^{7}LiF-NaF-BeF_2 for optimum spectrum and AnF_3 solubility.

Phase diagrams for these systems are shown in Fig. 12 (Meer, 2006 and Thoma, 1959). The curve that delineates the high-temperature region of the binary phase diagrams (in a composition versus temperature representation) defines the domains of stability of the liquid (at high temperatures) and of the solid or a mixture of solid and liquid (at low temperatures). The lowest melting temperatures for LiF-BeF_2 and LiF-NaF are about 352 °C (655 K) at the composition 48 LiF-52 BeF_2, and 652 ^{o}C (925 K) at the composition 60 LiF-40 NaF (mole%), respectively.

Table 4 describes properties of currently investigated molten-salt solvent compositions, where ρ is the density, C_p the heat capacity, η the dynamic viscosity, and κ the thermal conductivity. Note that these data are indispensable for a sound thermo-hydraulic (rheological behavior and heat conduction) assessment (Meer, 2006).

To have a better appreciation of what the issues are, let us consider the phase diagram of the binary molten salt, LiF-UF_4 shown in Figure 13. In this case, the lowest melting temperature is about 490 °C (763 K) in the system free of BeF_2 at the composition 73 LiF-27 UF_4 (mole%). The phase diagram for the ternary molten salt, LiF-BeF_2-UF_4, is shown in Figure 14. This system has two eutectics with compositions containing more than 1 mol% UF_4. One of these is at 713 °C (986 K) at the composition 70 LiF – 12 BeF_2 – 18 UF_4. The other is at 699 °C (972 K) at the composition 69 LiF – 23 BeF_2 – 8 UF_4 (Meer, Konings and Oonk, 2006).

The phase diagram for the binary molten salt, LiF-ThF_4, is shown in Fig. 15 (Meer, Konings and Oonk, 2006). The lowest melting temperature is about 570 °C in this system, with ThF_4 ranging between 22 and 28 mole%. The LiF-BeF_2-ThF_4 ternary phase diagram is shown in Figure 16 (Meer, Konings and Oonk, 2006).

We might want to avoid, or at least minimize, beryllium in the molten salt, and a pure LiF base composition for the salt because, as will be shown later, the solubility of Pu and REE trifluorides is higher in low-BeF_2 compositions. It is worth noting that the behavior of molten fluorides will be very much affected by appreciable concentration of fission products that will evolve with burn-up. Hence, it is imperative that optimum fuel composition be selected on the basis of validated thermochemical analyses carried out for a variety of salts. Of particular importance are

the following sets of candidate fluoride components {BeF_2, LiF, NaF, ZrF_4} with {ThF_4, UF_4, PuF_3, AmF_3}, and fluorides such as {CsF, KF, RbF}, in the presence of REE fluorides such as CeF_3 and LaF_3.

Vapor pressure over molten salt

This topic could have been of importance if we had chosen to employ molten salt facing the chamber, that is, a wetted wall or thick liquid wall chamber design. Even though this choice was not made, we include the vapor pressure information here because low vapor pressures at operating temperature are desirable for safety reasons and to minimize the load on the off-gas handling system. The vapor pressures of components A and B over a binary liquid solution $A_{1-x}B_x$, within the regular solution model description of the liquid phase, are given by (see Appendix)

$$p_A = p_A^0 \exp\left[\ln(x_A) + \frac{x_B^2}{RT}\Omega\right] \text{ and } p_B = p_B^0 \exp\left[\ln(x_B) + \frac{x_A^2}{RT}\Omega\right]$$

where p_i^0 is the vapor pressure associated with the pure component i, Ω is the interaction parameter that describes the mixing Gibbs energy of the liquid phase within the regular solution model (see Appendix A), R is the gas constant (*e.g.*, R=8.31451 J· mole^{-1}· K^{-1}), and T is the thermodynamic temperature.

For UF_4 and LiF, the vapor pressures of the pure liquid end members are given by:

$P_{UF_4-pure}(atm) = e^{-35236/T-5.03\cdot \ell nT+57.88}$ for the vapor pressure of UF_4 over pure UF_4 liquid (Kubachewki and Alcock, 1979);

and

$P_{LiF-pure}(atm) = e^{-33532/T-4.02\cdot \ell nT+47.63}$ for the vapor pressure of LiF over pure LiF liquid.

In the case of a liquid solution of LiF - UF_4, the vapor pressures of UF_4 and LiF over the liquid of the two components are given by Kaufman, Agren, Nell and Hayes, 1983):

$$P_{UF_4}(atm) = P_{UF_4-pure} e^{+\ell n(x_{UF_4})-7217\cdot x_{LiF}^2/T}$$

$$P_{LiF}(atm) = P_{LiF-pure} e^{+\ell n(x_{LiF})-7217\cdot x_{UF_4}^2/T}$$

where x_{UF_4} and x_{LiF} are the mole fractions of UF_4 and LiF, respectively, with $x_{UF_4} + x_{LiF} = 1$. The x^2 coefficient of –7217 corresponds to the interaction parameter, divided by the gas constant R, for the liquid LiF-UF_4 within the regular solution approximation (see discussion presented above). These data were assessed to reproduce, together with the Gibbs energy parameters that describe the solid phases, the experimentally determined LiF- UF_4 phase diagram.

For x_{UF_4}=0.3 and x_{LiF}=0.7 we obtain the vapor pressure versus temperature curves shown in Fig. 17. One can see that the vapor pressure is considerably reduced in the case of the binary liquid solution compared to the pure value as expected. The same information over a smaller temperature range is displayed in Fig. 18. The same curves are plotted over a smaller temperature range in Figure 19. The vapor curves extend over a considerable range of temperatures even below the point where the salt becomes a solid. While there is no discontinuity at the melt point the behavior below the melt point is not accurately treated nor is it of interest to us.

The vapor density over this melt is shown in Fig. 19, assuming ideal behavior in the vapor phase.

With the vapor pressures over the binary liquid being estimated for the LiF-UF_4 system, it was assumed that the same interaction parameter for the regular solution could be used as a first approximation for the LiF-ThF_4 system because this information is not available for this system. Data for pure ThF_4 were taken from Ref. (Darnell and Keneshea, Jr., 1958).

$P_{ThF_4-pure}(atm) = 10^{-15270/T+7.940}$ for the vapor pressure of ThF_4 over pure ThF_4 liquid.

In the case of a liquid solution of LiF- ThF_4, the vapor pressures over the liquid of the two components are given by:

$$P_{ThF_4}(atm) = P_{ThF_4-pure} e^{+\ell n(x_{ThF_4}) - 7217 \cdot x_{LiF}^2 / T}$$

$$P_{LiF}(atm) = P_{LiF-pure} e^{+\ell n(x_{LiF}) - 7217 \cdot x_{ThF_4}^2 / T}$$

where x_{ThF_4} and x_{LiF} are the mole fractions of ThF_4 and LiF, respectively, with $x_{ThF_4} + x_{LiF} = 1$

For x_{ThF_4}=0.275 and x_{LiF}=0.725 we obtain the vapor pressure versus temperature curves shown in Fig. 20. One can see that the vapor pressure is considerably reduced in the binary liquid solution compared to the pure values. The same information over a smaller temperature range is given in Fig. 21.

The vapor density over this melt is displayed in Fig. 22, assuming ideal behavior in the vapor phase.

Remember the curves for the vapor pressures over a LiF-ThF_4 solution are estimates based on the assumption that the interaction parameter for ThF_4-LiF is the same the same as for the UF_4-LiF system. This assumption will need to be verified.

The following shows how to calculate the flux of ThF_4 or LiF molecules and the density:

$$J = \frac{n\bar{v}}{4} = CPT^{-0.5} \qquad C = \frac{1}{(2\pi mk)^{0.5}} \qquad n = \frac{P}{kT}$$

$$m_{ThF_4} = (232.04 + 4 \times 18.998) \times 1.6605 \times 10^{-27} = 5.11 \times 10^{-25}\ kg$$

$$m_{LiF} = (6.941 + 18.998) \times 1.6605 \times 10^{-27} = 4.307 \times 10^{-26}\ kg$$

$$C_{ThF_4} = \frac{1}{(2\pi \times 5.11 \times 10^{-25}\ kg \times 1.38066 \times 10^{-23})^{0.5}} = 1.50 \times 10^{23}$$

$$C_{LiF} = \frac{1}{(2\pi \times 4.307 \times 10^{-26}\ kg \times 1.38066 \times 10^{-23})^{0.5}} = 5.173 \times 10^{23}$$

In conclusion, capabilities are in place to predict the vapor pressures of various combinations of molten salts, which should prove to be useful in the future to show that specific mixtures of molten salts meet the demand of a low vapor pressure at operating temperature in a LIFE engine. We have shown through two examples, LiF-UF_4 and LiF-ThF_4 that the vapor pressures are quite low in the temperature range relevant to the operation of a molten-salt-fueled LIFE engine.

Solubility of Plutonium and Rare-earth Elements

The solubility of the transuranic (TRU) elements, particularly Pu, as well as the rare-earth elements in molten salts has to be considered because as a function of burn-up a substantial quantity of fission products will be generated (cf. section on *Neutronic Performance*). The solubility of PuF_3 in a salt mixture based on LiF-BeF_2 has been recognized as a possible issue, and the high melting point of PuF_3 is the likely source of the low solubility problem, cf. Table 5.

The results of the studies performed by Barton and others at ORNL in the 50's and 60's during the MSRE program (Barton and Stehlow, 1958 and Barton, 1960) and confirmed in the 70's by

Mailen *et al., 1971* on LiF-BeF_2, have shown that the solubility of PuF_3 in fluoride salt melts is both composition and temperature dependent, as shown in Figs. 23-26. More recent studies conducted at the Kurchatov Institute in Moscow (Russia) (Ignatiev et al., 2003) have reported much higher PuF_3 solubilities (about 30 and 40% higher than the Barton, 1960 and Mailen, et al., 1971 results, respectively) as shown in Table 6 and in Fig. 26, and the discrepancies were attributed to samples held for a longer time at temperature before analysis.

The high melting point of PuF_3 is the source of the low solubility problem. Recent modeling studies conducted at ITU (Karlsruhe, Germany) based on experimental data from Barton and Strehlow, 1958 and Barton, 1960 have shown that a solubility of 1.3 mole% of PuF_3 could be achieved in a series of molten salts, as shown in Table 7, although for binary salts the solubility of PuF_3 is higher in LiF-BeF_2 than in NaF-BeF_2 (at 565 ^oC) as shown in Figures 27 and 28.

The thermal, physical, and neutronic properties of a variety of candidate base compositions for molten salts (as well as relevant elemental constituents) are given in Table 8.

As an example, the range of existence of a liquid phase at 550 ^oC (823 K) in the case of LiF-NaF-BeF_2, with 1.3 mole% PuF_3 is shown in Fig. 29.

From recent studies conducted at Institute for Transuranium Elements (ITU) in Karlsruhe (Germany), it is clear that the solubility of Pu in molten salt reasonably well understood, and with additional experimental data on a few specific salt mixtures that would validate thermodynamic modeling, optimal molten salt composition could be selected.

The chemistry of the rare earth elements (REE) and the related element, yttrium (Y), in molten fluoride salts with relevant compositions is less well known. These elements, particularly the light REE (LREE) have large fission yields, and constitute a large fraction of the fission products produced in a U- or Pu-fueled fission blanket (cf. Fig. 9). The trivalent REE, particularly the light REE, have the same valence, and are similar in ionic radius to the +3 valence actinides that lie below them in the periodic table, and would be expected to have similar chemical behavior. Indeed, studies carried out for CeF_3 and NdF_3 have shown that their addition to molten salts consistently reduces the solubility of PuF_3 solubility on approximately a 1-for-1 molar basis, as shown in Figures 30 and 31. This suggests that the trivalent REE and Pu3+ have approximately ideal mixing behavior in these melts. Furthermore, the trivalent REE form trifluorides that are isostructural with PuF_3, and form a complete (Pu, REE)F_3 solid solution in which the Pu/REE ratio is approximately that of the melt, indicating that mixing in the solid phase is also approximately ideal. The large fission yield of the light REE and Y therefore further constrains the selection of an appropriate salt composition, and, as discussed in an earlier section, will require on-line processing to remove them so the solubility of a (Pu, REE)F_3 solid is not exceeded during the operation of the LIFE engine.

In contrast, addition of divalent REE (e.g., Eu^{2+}, and Sm^{2+}) has negligible effect on the solubility of Pu^{3+}, as would be expected from their different charges and radii (Ignatiev et al., 2006).

Trivalent yttrium is also known to form a stable fluoride with Li: $LiYF_4$, and the intermediate-mass REE (those with masses > Eu) also form mixed $Li(REE)F_3$ solids. No information has been found related to the solubility of these solids in fluoride melts of the compositions likely to be used for a molten salt for a LIFE engine. Although the fission yields of these elements are lower than those of the LREE, data will be needed to assess the solubility of such phases and to assure that they do not precipitate in the molten fuel. In any event, a processing scheme that removes the REE will also remove Y so this issue will naturally be addressed by whatever method is adopted to control the concentration of REE.

Processing and clean up

Some fission products in a molten salt reactor are removed almost automatically and some can be removed by applying processes to side streams (Engel et al., 1980). In addition it will be necessary in any molten salt system to "clean up" or "doctor" the molten salt to remove impurities such as oxygen, and to maintain the appropriate fluorine (redox) potential in the salt. Hydro-fluorination is commonly used to remove moisture. The salt is kept reduced to control corrosion of structural materials by keeping the ratio of $UF_3/UF_4 \approx 0.05$ as a buffering agent.

Gas sparging

Bubbles of inert gas, He, are injected into the molten salt flow. This serves to sparge gaseous fission products, as well as some of the more volatile fluorides. In this way ^{85}Kr ($T_{1/2}$ = 11 y), ^{133}Xe ($T_{1/2}$ = 5.2 d), and ^{135}Xe ($T_{1/2}$ = 9.1 h) are removed in an estimated time of 50 s (Engel et al. 1978). These gases are held up on beds of activated charcoal (or a zeolite) and allowed to decay to stable ^{85}Rb and ^{133}Cs, and long-lived ($T_{1/2}$ =2.3 x 10^6 y) ^{135}Cs. This last nuclide would need to be combined with the alkali waste stream from the final processing of the molten salt at the end of the engine's life and immobilized in a waste form for disposal in a repository. Tritium should be separated from the gas stream prior to contact with the graphite bed. Some form of active cooling of the charcoal beds will be necessary in order to remove the heat generated by decay of the trapped fission products. The half-life of ^{85}Kr is sufficiently long that on-site decay during the operational period of a LIFE engine will not suffice to reduce its activity to inconsequential levels. Therefore, the ^{85}Kr will need to be stripped from the graphite, concentrated, and sent to some form of long-term decay storage. Any tritium present in the sparge gas will also need to be separated and sent to the tritium handling facility for further processing and purification.

Noble and semi-noble metal extraction

The noble and semi-noble metal fission products do not form soluble fluoride complexes at the fluoride potential of the melt and are insoluble. They are: Zn, Ga, Ge, As, Nb, Mo, Tc, Ru, Rh, Pd, Ag, Cd, In, Sn, and Sb. Experience with the ORNL Molten Salt Reactor Experiment (MSRE) suggests that these elements form multi-atom metallic clusters in the melt (Compere et al., 1975). In the MSRE, some of these elements were removed as particulates in the sparge gas, some plated out on the metal walls of blanket structures and piping and heat exchangers, and the remaining fraction circulated in the molten salt. The proportion of these elements in each of these reservoirs varied unpredictably during operation of the MSRE, and additional study of the chemical behavior of these elements will be needed.

If these elements circulate many times around the pumped circuit before plating out it may be possible to preferentially capture them on filters in a slipstream process loop in a time estimated at 2.4 h. One suggestion is to pass the molten salt through a nickel wire filter where plating occurs. Another suggestion is to use a centrifuge to enhance or concentrate these elements. This would be effective if precipitation is occurring homogeneously throughout the molten salt, so that these elements are present in the salt as solid metallic particles of appreciable size. If, however, precipitation were occurring preferentially heterogeneously at metal surfaces, or if, as suggested by the MSRE experience, the particles are nanometer-sized aggregates (Compere et al., 1975), then centrifugation would not be effective. We need to consult those more familiar with the problem to make a prediction of which mechanism is most operative.

Cowell et al. 1995 suggested electro-winning as a means to remove the noble and semi-noble metals from the fluoride salt blanket of an accelerator-based conversion (ABC) scheme for transmuting surplus Pu. Electro-winning is commonly used in industry (e.g., it is the sole commercial method for producing aluminum) to yield pure metals from oxide or halide feed materials that have been dissolved in a molten salt. In the case of LIFE, we are interested in the inverse problem, namely the cleanup of a molten salt rather than the production of a pure metal. In the case of a Be-containing salt (e.g., flibe), the electro-winning system would use an electrochemical cell consisting of a consumable anode fabricated from metallic Be, and a Ni cathode onto which the noble/seminoble metals and zirconium are plated. The reaction that describes the process is

$$n\ Be(s) + 2\ MF_n(salt) = n\ BeF_2(salt) + 2\ M(s)$$

So long as the free energy difference between BeF_2 and MF_n is negative, this reaction will be spontaneous, thus, the cell could be operated passively. Cowell et al., 1995 further suggested that the application of an externally generated potential difference between the electrodes would enhance the rate of mass transfer. The electrochemical potentials of plutonium, other actinides, and lanthanides lie between those of beryllium and lithium, so this process will not remove these elements from the molten salt. In addition to removing fission product metals, the cell could also provide control of the redox potential of the fuel salt.

These elements would then be in metallic form, and ready to be converted to an appropriate waste form discussed in a subsequent section.

Removal of other fission products

The remaining fission product classes form stable fluorides and will circulate in the molten salt. At a minimum, it appears that it will be necessary to remove the REE fission products (plus yttrium) so that the solubility limit of a (Pu, REE+Y)F_3 solid solution is not exceeded. A second requirement is that the processing scheme should leave the actinides in the fuel salt, or, failing this, be designed so that the actinides are removed together from the salt, and can be easily reinjected back into the salt for continued burning. Removal of the fission products other than the REE (and those discussed above) would improve the neutron economy of the engine, but does not appear necessary from either a chemical or a neutronics perspective. This makes the processing requirements for LIFE considerably less stringent than previous molten salt reactor systems, which usually needed to remove fission products to reduce the parasitic absorption of neutrons so criticality could be maintained. Molten-salt breeder reactors had the additional need to extract ^{233}Pa from the core to allow decay into fissile ^{233}U without transmutation to ^{234}Pa; the ^{233}U was then returned to the core.

There are several possible approaches to processing the salt to remove fission products, and three of the most promising are discussed below. Because considerable research on processing has been done in the past, we need to further study the literature to search for processes that could be adapted to processing for LIFE. This topic should be one of the high-priority future research items for a LIFE program. Note also that because of the inclusion of molten-salt-fueled reactors as one of the Gen-IV technologies, there is an upsurge of interest in developing on-line processing systems for molten salts. (Most of this activity is in Europe and Russia.) For instance, in 2008, the French Commissariat à l'Énergie Atomique (CEA) has plans to design and assess conceptual flow sheets for the processing of a thorium-fueled molten salt reactor (Cabet et al., 2008. The LIFE effort should be able to leverage the results generated from this new work on Gen-IV systems.

Depending on the process chosen, it might be possible to modify the system to allow removal of weapons-useable materials, and so raises questions as to how well a LIFE engine with on-line processing meets the proliferation-resistance goals for LIFE. In the case of burning weapon Pu this consideration does not apply because the proliferation risk is highest at the initial state of the system; even with on-line processing, the proliferation risk of an operating Pu-fueled LIFE engine is much less than that of the original separated weapons-grade Pu.

Reductive extraction

Perhaps the most mature of the three processing approaches discussed here is the one based on the reductive extraction of metals from the salt into a molten metal, such as Bi or Cd, that

contains a reductant, typically an alkali metal such as Li. The molten salt reactor program developed several extraction schemes using this technology, and tested them at the bench scale (Engel et al, 1980 and Engel et al., 1978). The program also conducted an associated engineering effort to build and test the equipment necessary for practical application of the method on a molten salt reactor. More recent work in this area has been done for the electrometallurgical processing system developed at Argonne National Laboratory for the Integral Fast Reactor and the Experimental Breeder Reactor programs (National Research Council, Electrometallurgical Techniques). Partitioning data for many, but not all, of the elements of interest are available for extraction into molten Bi with variable amounts of Li added as a reductant. This process can be described by the reaction:

$MF_n(salt) + n\ Li(Bi) = M(Bi) + nLiF(salt)$,

where MFn is a metal fluoride dissolved in the molten salt. This process can remove noble and semi-noble metals, the actinides, Y, the REE, and Zr (see Fig. 32). Divalent and monovalent alkalis and alkaline earths are removed to a much lesser extent.

In the LIFE application, we are primarily interested in removing fission product REE from the salt, while leaving the actinides and other fission products in the salt so they can be transmuted. This may be possible using a relatively simple scheme of sequential extraction of the actinides (except Th, which has partitioning behavior more like the REE) into molten Bi:Li, followed by extraction of the REE and Th into a separate reservoir of molten Bi:Li with a higher content of Li. The separated actinides and Zr would be electrolytically transferred from Bi:Li back into the fuel salt. The REE (along with any alkalis and alkaline earths that are present) can then be selectively extracted from the Bi:Li stream containing the REE+Th by contacting the liquid metal with a molten LiCl salt (Fig. 33). Although the mass removal rate of the REE via this process would be rather low, due to the low concentrations of REE dissolved in the transfer fluids, continuous or semi-continuous operation of such a system should suffice to keep up with the production of REE by fission in an engine. Higher separation efficiencies could be achieved by using multiple countercurrent extractors at each of the separation steps.

Under the redox conditions of a molten salt fuel, the solubility of Bi in flibe is very low (on the order of 1 ppm), so that Bi contamination of the fuel salt should be negligible (Rosenthal, Haubenreich and Briggs, 1972). It may be necessary to impose a fluoride-removal process on the Bi stream flowing from the fuel salt contactor to the LiCl contactor because contamination of the LiCl salt with fluoride was found to reduce the separation of Th from the REE in this step (Ferris, Smith, Mailen and Beli, 1972). Similarly, it may be necessary to have a chloride removal process for the return flow of Bi to the fuel-salt contactor so that the fuel salt is not contaminated with chloride.

Any noble or semi-noble metals not removed by the cleanup process described in the previous section would strongly partition into the metal phase in the first metal extraction step; indeed,

they could be removed with high efficiency simply by contacting the molten fuel salt with molten Bi containing no Li reductant in an extraction step preceding the actinide-extraction step.

A simplified conceptual flow sheet for this process is shown in Figure 34. At this point, this separation scheme purely notional, and a serious experimental program to obtain partitioning data using the salt composition(s) selected for a molten-salt LIFE engine would be needed to make a quantitative assessment of the separations efficiency and possible process pitfalls. Furthermore, key partitioning data are not available at all for some elements (e.g., Pu^{3+} partitioning between Bi:Li and LiCl). Nevertheless, the relatively large body of literature related to this technology, and the extensive (but aging) experience base, makes this an attractive option for further near-term study.

Electrochemical methods

As an alternative to the reductive metal transfer process, the possibility of developing a purely electrochemical separations system should be investigated. Such a system would be an augmentation of the electro-winning concept discussed above for the removal of the noble and semi-noble metals from the salt. The advantage of this approach is that electrochemical manipulation of the system introduces no new "reagents" (i.e., molten metals or salts) into the system, thus minimizing the potential for contamination of the fuel salt with undesired elements. Because the reduction potentials of the REE lie between those of the actinides and Li or Be, the actinides would need to be electrochemically removed before the REE could be removed. The separated actinides would be redissolved (by fluorination or by anodic dissolution) back into the fuel salt. The REE would be removed either electrochemically, or by precipitation as oxides (see below). A conceptual flow sheet for an electrochemical separation scheme for the REE is shown in Figure 35 (Ignatiev, Gorbunov and Zakirov, 2004). Note that the actual removal of the REE from the fuel salt in this scheme is done by oxidation with Li_2O rather than electrochemically.

Oxide Precipitation

The use of a chemical oxidant (e.g., Li_2O or other alkai/alkaline earth oxides) to separate the actinides and REE by sequential precipitation from molten fluoride salts has also received some consideration in the past (Rosenthal , Haubenreich and Briggs, 1972 and Ignatiev, Gorbunov and Zakirov, 2004). An advantage of this approach is the simplicity of the equipment needed, and less stringent materials corrosion requirements for the equipment. The limited experimental investigations conducted to date, indicate that upon incremental addition of an oxidant, the actinides are first to precipitate as oxides followed by the REE. This means that as with the previously discussed methods, the first step in the process for removing the REE involves the removal of the actinides from the fuel salt. It is therefore not clear that a processing system based on oxide precipitation would have a compelling advantage over the reductive metal process or an electrochemical process.

End-of-life processing of molten salt fuel

Given that Li and Be salts of fluorine are water-soluble, the flibe salt itself will not be a waste form suitable for disposal in a geologic repository. Processing of the salt at the end of the life of a LIFE engine will therefore be necessary. It is possible that the processes used for the on-line treatment of the molten salt during the operation of the engine can be modified or adapted to do the final processing of the salt. The main goals of this processing will be to reduce the volume of the waste stream requiring long-term isolation by separating the non-radioactive flibe salt from the remaining fission and activation products. The cleaned-up salt could potentially be recycled for use in other engines. Removal of the bulk of the fluoride salt will also have the effect of reducing the number of neutrons produced by (alpha, n) reactions on ^{19}F, which could greatly complicate the shielding requirements for the waste.

Waste streams from processing

Because the processes that will be used for the on-line and end-of-life processing have not been determined, it is difficult to be specific about the nature of the waste streams resulting from these processes. Nevertheless, one can guess that they will be similar to those of the electrometallurgical process developed by Argonne National Laboratory (ANL) for a variety of spent nuclear fuels (National Research Council, Electometallurgical Techniques). One might therefore expect the waste streams from a LIFE engine to include a metallic waste stream containing Zr and the noble/semi-noble metals (*e.g.*, Mo, Nb, Ru, Rh, Ag, Cd, Tc), and at least one additional waste stream containing the REE, along with some actinides, alkalis, and alkaline earths. The chemical form of this second waste stream is not well defined – most likely it would be a fluoride or chloride stream; however it could be an oxide stream or some other material, depending on the nature of the processing used. In the case of the ANL electrometallurgical process, this stream consisted of a chloride salt.

In addition to these two (or more) streams, there will be the waste stream generated by the offgas treatment process. As discussed above, the radioactive noble gases sparged from the molten salt during operation will either decay to stable isotopes of Rb and Cs, or to long-lived ^{135}Cs, which will need to be separated and combined with the alkali-containing waste stream generated by direct treatment of the salt. The offgas will also contain some quantity of other chemical species that have high vapor pressure in molten fluoride salts (*e.g.*, ZrF_4, I_2), as well as entrained particles of salt.

Waste forms suitable for disposal

Assuming the waste streams outline above, one can further assume that one of the final waste forms from a molten-salt-fueled LIFE engine will be a metallic alloy. For the metal waste form resulting from their electrometallurgical process (which was already Zr-rich due to the presence of Zircaloy cladding hulls in this waste stream), ANL added additional Zr to produce a lower melting point alloy, and to improve the corrosion behavior of the alloy under repository

conditions. At this point, one cannot predict what types of further processing will be needed to convert the metallic waste stream into an alloy that has good performance characteristics as a waste form. This will only be possible once process flow sheets and material balance estimates are available for proposed processing systems for a molten-salt LIFE engine. Nevertheless, the development of a suitable metallic waste form should be a relatively straightforward matter.

The waste stream containing the REE, actinides, alkalis, and alkaline earths is more problematic than the metal waste form. If a process similar to that shown in Figure 34 is used, in which the REE are separated into a LiCl salt, then the process used for converting chloride salt waste stream of ANL electrochemical process to a form acceptable for disposal in a repository could be adapted for this waste stream (Dexa 1999). The ANL process involved occluding the molten chloride salt within the channels and cages of an alumino-silicate zeolite, then mixing this "salt-loaded" zeolite with a borosilicate glass frit, and sintering the mixture in a hot isostatic press. The resulting waste form consists of a multi-phase, glass-bonded ceramic. If the REE stream consists of a fluoride salt, however, this approach is unlikely to work. Molten fluoride salts are not compatible with silicates, due to the formation of stable (and highly volatile) SiF_4. A silicate or aluminosilicate dominated waste form is unlikely to be possible for LIFE wastes unless the waste stream is first processed to remove the bulk of the fluoride. Although there are fluoride-containing crystalline silicates, and some level of fluoride can be tolerated, the presence of fluoride in a silicate glass waste-form will severely degrade the long-term performance of the glass.

Little work has been done on developing waste-forms for fluoride salt waste streams, and there are many options that could be explored for immobilizing either a fluoride salt, or a fluoride-contaminated oxide waste stream. The possibility of reacting the fluoride salts with phosphate-, titanate-, or zirconate-containing precursors to produce suitable phosphate (e.g., monazite, apatite (Dexa, 1999 and Donald et al., 2007), titanate (e.g., pyrochlore, hollandite), or zirconate (e.g., fluorite-structure REE-zirconate) phases should be explored. If the fluoride salt is first converted to an oxide, then production of either a glass or a multi-phase ceramic involving the above-mentioned phases would be a straightforward extension of previous work. These, and related, phases are known to accept actinides, REE, and alkaline earths into their structures, and have a history and relevant scientific literature to draw upon. More speculative possibilities that might be produced directly from a fluoride salt, but for which there are little literature data, include such exotic phases such as hsianghualite (nominally $Ca_3Li_2Be_3(SiO_4)_3F_2$), semenovite (nominally $(Ca,Ce,La,Na)_{10\text{-}12}(Fe{+}{+},Mn)(Si,Be)_{20}(O,OH,F)_{48,}$ nareniobsite ($NbNa_3Ca_3(Ce,La)(Si_2O_7)_2OF_3$), and a host of other naturally occurring mineral phases. Clearly, the possible chemistry is rich, and poorly explored to date. Unfortunately, this also means that the *de novo* development and qualification of a completely novel waste=form will take more time than following a previously explored path.

Economic prospects

An Excel-based systems code is being developed for TRISO-fueled version of LIFE. The code contains costing for all the major subsystems including fission fuel fabrication, fusion fuel targets, laser, engine, power conversion and other balance of plant systems, and end-of-life spent fuel storage and disposal. Work will be needed to add subsystems and features unique to the molten-salt version of LIFE so that systems can be compared on a consistent basis. We are considering various figures of merit by which to evaluate the attractiveness of various LIFE designs and to compare the LIFE concept to other future energy systems. An open question is how to properly credit LIFE for its ability to destroy weapons Pu or long-lived waste from SNF. For example, if the estimated cost of electricity is higher than competing options, the additional operating cost can be assigned to the material destruction mission. In that way, one can calculate the cost per unit mass destroyed. This cost can be expressed in dollars per ton of Pu burned and compared to other proposed uses or disposition pathways for this Pu, such as burning in LWRs as mixed oxide fuel (MOX).

Safety issues

Safety studies will be conducted in the future.

Chapter C. Gaps in Knowledge and System Vulnerabilities

The opportunities offered by molten salts as candidate fuels in general, and more specifically in the context of LIFE, Gen-IV and the thorium cycle option, should lead to increased interest. Future studies should be undertaken in five areas: fuel salt chemistry, design and safety, reactor physics, fuel salt clean-up (salt control, online processing and reprocessing, waste form and waste disposal), and materials mechanics and corrosion.

Additional burnup calculations are needed to assess and optimize the performance of a molten-salt-fueled LIFE engine for burning weapons-grade Pu, HEU, and spent nuclear fuel. The possibility of steady-state operation of the engine needs to be assessed for each of the potential fuel types.

An integrated materials design and testing facility will be required to make an optimal choice of salt for the LIFE engine. Salt chemistry, corrosion chemistry, and alloy selection should be jointly studied, and the establishment of a coordinated effort with other activities carried out for the Gen-IV molten-salt fueled reactor should be considered. The radiation damage lifetime of the graphite moderator must be assessed. In next year's work we need to develop the design in the direction of steady state operation allowed by having processing of fission products.

A thermodynamic database that includes the following fluoride salts: {AmF_3, BeF_2, CeF_3, CsF, KF, LaF_3, LiF, NaF, PuF_3, RbF, ThF_4, UF_4, ZrF_4} is being established to further quantify solubility of fission products in the salt, and perform materials assessment to optimize salt composition that satisfies the requirements of the LIFE engine. The thermodynamic modeling is carried out in the framework of the CALPHAD approach (Sanders and Miodownik, 1998, Miodownik, 1994, MRS Bulletin, Vol 24, 1999, Kaufman and Bertnstein, 1970 and CALPHAD, 2002), and the Thermo-Calc software, 1958) is used to perform the equilibrium calculations and the assessments. As of mid-August the data that have been assembled are summarized in Table 9. Most of the data originate from published work performed at ITU (Karlsruhe, Germany) that is summarized in Appendix B.

*** Develop an updated fission-product removal system flow sheet that is compatible with all goals of the LIFE engine.

*** Evaluate LIFE-molten salt engine global fuel cycle with the objective of minimizing the global, chemically separable, weapon-usable fissile inventory.

*** Identify and quantify potential installation vulnerabilities for bypassing safeguards.

*** Assess long-term economic and environmental acceptability.

An integrated processing system for the on-line processing of the salt fuel must be designed and assessed. This system will need to be include: (1) the He-gas sparging system; (2) a process for

removing the noble and semi-noble metals; (3) a process for removing REE; (4) a system for "scrubbing" the fuel of oxygen and other undesirable contaminants; and (5) a system for controlling the fluoride (redox) potential of the salt. It is recommended that contact be made with established groups at Argonne National Laboratory and Oak Ridge National Laboratory that have experience in the pyrochemical processing of salts. Links should also be made with the groups in Europe and Russia that are actively working on the Gen-IV molten-salt reactor option.

The difficulty of modifying the fuel processing system(s) to allow diversion of weapons-useable fissile material must be assessed in terms of the proliferation risks relative to other nuclear energy options.

Once the composition of the fuel salt and the envelope of likely processing systems (and their associated waste streams) have been established, a program to develop waste forms suitable for final disposal needs to be established.

Zr has a low melting point (sublimation) and is likely to have a fairly high vapor pressure as ZrF_4. This might allow removal by distillation, though reductive extraction into a molten metal (e.g., Bi) containing an alkali reductant would also be effective (see processing discussion below). In future studies we can get vapor pressure data. The low melting point of ZrF_4 should lower the eutectic temperature of the salt, and should increase Pu solubility at a given temperature.

Melting temperatures of NpF_3, AmF_3, and CmF_3 are needed; however, their concentrations are so much lower than Pu that these data are probably not of great importance.

Tm, Yb, and As are not in the neutronics calculation data base and hence some small errors may have resulted.

BaF_2, SrF_2 and YF_3 have high melting points and high concentrations. Y, which has chemistry similar to the intermediate-mass REE, should be removed in any on-line processing system designed to remove the REE. Ba and Sr removal may be possible, but does not appear to be necessary from a neutronics or solubility standpoint.

Chapter D. Strategy for Future Work

Estimates of mol fractions to use in phase diagrams and solubility plots for the molten salt fuel LIFE engine

Based on prior neutronics transport calculations and solubility estimates at 600 °C of 1 mol% of PuF_3 we suggest as a trial an 18% Th and 6% U salt formulation. The Pu concentration starts at zero but after a few years the Pu builds up to a quasi-steady state value. Early in the burn the quasi-steady state salt formulation is as follows:

$$0.75\ LiF + 0.18\ ThF_4 + 0.003\ UF_3 + 0.057\ UF_4 + 0.01\ PuF_3$$

As Li, Th and U atoms are removed we assume they are replenished. Note the U is kept in a partially reduced state with about 5% in the +3 state.

In about 60 years of operation the two remaining fission products, Zr and Ba build up nearly linearly to 2.9 and 2.2 mol% based on prior neutronics calculations. We assume many of the fission products are removed as they are produced, especially the rare earths that would otherwise limit solubility. The salt formulation at 60 years would be:

$$0.699\ LiF + 0.18\ ThF_4 + 0.003\ UF_3 + 0.057\ UF_4 + 0.01\ PuF_3 + 0.029\ ZrF_4 + 0.022\ BaF_2$$

For discussion purposes let us assume a spherical blanket whose first wall is at 2.5 m radius, with a 0.15 m beryllium pebble zone out to 2.65 m radius and a 0.5 m molten salt zone out to 3.15 m radius. This zone might contain graphite. We take two cases: graphite by volume of 0 and 75%. The molten salt volume for these two cases would be 53 and 13 m^3. If we process at the rate of 76 m^3/y we could keep the rare earths limited to 0.1 mol% for the no graphite case and four times slower for the graphite case.

Based on the available thermodynamic information that was collected in a thermo-chemical database (cf. Appendix B) CALPHAD modeling was applied to the determination of the melting point as a function of the ratio Th/(Th+U) to identify the optimal ratio at which the melting temperature of the salt mixture is minimum. For this determination a complex mixture of varying composition made of {LiF, PuF_3, ThF_4, UF_4} was considered. Since no thermodynamic data at the present time exist for UF_3, it was assumed that UF_4 and UF_3 were behaving in the same way. In addition, although the 6 combinations resulting from the 4 fluoride components have been fully validated, it was assumed that no additional energetic terms exist for describing the 4 ternary combinations. Under these assumptions and with the compositions given in Table 8, the results are presented in Fig. 36.

According to Fig. 36, there is an optimal ratio Th/(Th+U) around 0.62 that guarantees a minimum melting temperature of 520 ^{o}C, *i.e.*, with the following salt formulation: 0.745 LiF + 0.15 ThF_4 + 0.09 UF_4 + 0.015 PuF_3. At a late burn-up stage, similar calculations would require a more complete thermo-chemical database than the one presently available (cf. Appendix B). Once data will be collected for this more complete salt formulation {BaF_2, LiF, PuF_3, ThF_4, UF_4, ZrF_4} we will be in a position to represent the time evolution of the molten salt and predict the minimum temperature at which the salt of varying composition can operate in the liquid phase. Avoiding freezing anywhere and especially precipitation of Pu is the primary consideration for the minimum temperature in the loop. Thermal/hydraulics studies are needed to determine the maximum temperature in the molten salt loop. The maximum temperature is of great concern to materials properties.

Summary

We have considered substituting molten salt containing the same actinides that the TRISO fuel mission was considering in a very preliminary study. The nuclear performance seems to be somewhat better than the TRISO fuel case because of the removal of neutron absorbing fission products. Corrosion of the structural steel is mitigated by use of nickel or tungsten plating. As actinide fluorides primarily PuF_3 and rare-earth fluorides build up they exceed their solubility limit of about 1 mol%. The separation and removal of these rare-earth elements will be needed. The neutronics performance is better than for the TRISO fuel case because removal of neutron absorbing fission products based on current simulation results. Also processing allows continuous feed of materials and steady operation that will improve economics. These processes need more study especially the impact on nonproliferation assessment. Can LIFE goals still be sufficiently met with the molten salt design is a key unanswered question. We call for more study of the solubility and processing question that will go hand in hand with the blanket design and optimization. The cost of the molten salt option has not been estimated but is planned for next year.

Acknowledgements

Work by Peter Song on neutronics is appreciated. Jeff Powers carried this work on and made extensive case studies reported on here under support of the Lawrence Livermore National Laboratory Summer Employment Program. Work performed under the auspices of the U.S. Department of Energy by Lawrence Livermore National Laboratory under Contract DE-AC52-07NA27344.

Bibliography

A Technology Roadmap for Generation IV Nuclear Energy Systems (2002). www.ne.doe.gov/geniv/documents/gen_iv_roadmap.pdf

R. Abbott, "Thermal and mechanical design of the LIFE Engine," to be published in *Fusion Science and Technology* (2009).

C. E. Bamberger, R. G. Ross, and C. F. Baes, Jr., **"**The oxide chemistry of Plutonium in molten fluorides and the free energy of formation of PuF_3 and PuF_4", J. of Inorg. Nucl. Chem. **33**, 767-776 (1971).

C. J. Barton and R. A. Strehlow, "Solubility of PuF_3 in Alkali Fluoride-Beryllium Fluoride Mixtures", p. 84-88, in H. G. MacPherson, "Molten-salt reactor program – Quarterly progress report for period ending June 30, 1958", ORNL-2551 (February 1958) (120 pages)

O. Benes and R. J. M. Konings, private communication (August 2008).

O. Benes and R. J. M. Konings, private communication (August 2008).

J.P. Blanchard, C.J. Martin, "Thermomechanical effects in a laser IFE first wall,"J. Nucl. Mater. 347 (3) (2005) 192-206.

C. Cabet, O. Conocar, O. Koberl, C. Renault, N. Simon, C. Thévenot, Status of French programs on liquid salts and MSR –situation at CEA. Presentation at ALISIA Information Day, Paris, France March 4, 2008.

"*CALPHAD and Alloy Thermodynamics*", ed. by P. E. A. Turchi, A. Gonis, and R. D. Shull (TMS Publication, Warrendale, PA, 2002); and references therein.

E.T. Cheng, "Actinide-Burning Fusion Power Plants," *Fusion Science and Technology*, **47**, pp.1219-1223 (2005). E.T. Cheng, "Considerations for Fusion Based Actinide Destruction," *Fusion Science and Technology*, **44** (2003); also see references cited in this paper.

B. B. Cipiti et al., "Fusion Transmutation of Waste: Design and Analysis of the In-Zinerator Concept," Sandia Report SAND2006-6590, (Nov 2006). Also see J. D. Smith et al., "The role of Z-pinch fusion transmutation of waste in the nuclear fuel cycle," SAND2007-6487.

E. L. Compere, S.S. Kirslis, E.G. Bohlmann, F.F. Blankenship, W.R. Grimes, Fission-Product Behavior in the Molten-Salt Reactor Experiment, ORNL-4865 (1975).

Ralph Condit, private communication, June 25, 2008. Also see Pyrochemical processing technical data package, Vol 7. Chlorination. L-13966, R. Condit and C. Cate, Sept. 1991.

Cowell, B.S. ; Fontana, M.H. Krakowski, R.A. ; Beard, C.A. ; Buksa, J.J. ; Davidson, J.W. ; Sailor, W.C. ; Williamson, M.A. *Accelerator-based conversion (ABC) of weapons plutonium:*

Plant layout study and related design issues. Los Alamos National Lab., NM LA-UR-95-1096, 1995.

J. Darnell and F. J. Keneshea, Jr., "Vapor pressure of thorium tetrafluoride," NAA-SR-2710 Report from the Atomics International Division of North American Aviation, Inc., 1143-1145 (September 01 1958).

I.W. Donald, B.L. Metcalfe, S.K. Fong, L.A. Gerrard, D.M. Strachan, R.D. Scheele, A glass-encapsulated calcium phosphate wasteform for the immobilization of actinide-, fluoride-, and chloride-containing radioactive wastes from the pyrochemical reprocessing of plutonium metal. J. Nucl. Mat 361, 78-93 (2007).

L. Dexa, Preparation and physical characteristics of a lithium-beryllium-substituted fluorapatite. Metal. Mat. Trans. A, 30A, 147-153 (1999).

J. R. Engel, H. F. Bauman, J. F. Dearing, W. R. Grimes, E. H. McCoy, and W. A Rhoades (1980), "Conceptual design characteristics of a denatured molten-salt reactor with once-through fueling," Oak Ridge National Laboratory report ORNL/TM-7207, July (1980).

J. R. Engel, H. F. Bauman, J. F. Dearing, W. R. Grimes, E. H. McCoy, and W. A Rhoades (1980), "Conceptual design characteristics of a denatured molten-salt reactor with once-through fueling," Oak Ridge National Laboratory report ORNL/TM-7207, July (1980).

J. R. Engel, H. F. Bauman, J. F. Dearing, W. R. Grimes, E. H. McCoy, and W. A Rhoades (1980), "Conceptual design characteristics of a denatured molten-salt reactor with once-through fueling," Oak Ridge National Laboratory report ORNL/TM-7207, July (1980).

1. R. Eykens, J. Pauwells and J. Van Audenhove, "The hydrofluorination of uranium and plutonium," Nuclear Instruments and Methods in Physics Research A236 (1985) 497-499.

J. Farmer, N. Brown, R. Moir, H. Shaw and W. Halsey, "Options for Burning LWR SNF in LIFE Engine," internal report, LLNL (2008).

L.M. Ferris, F.J. Smith, J.C. Mailen, M.J. Bell, Distribution of lanthanide and actinide elements between liquid bismuth and molten LiCl-LiF and LiBr-LiF solutions. J. Inorg. Nucl. Chem., 34, 313-320 (1972).

R. Foster, R. L. Wright, Jr.: Chapter 4, Nuclear Reactions, Fusion, Chapter 11, Radiation Damage and Reactor Materials, Dispersion-Type Alloys (TRISO), Chapter 13, Nuclear Reactors, Molten Salt Breeder Reactor, Fusion by Laser, Fusion-Fission Symbiosis, Table 13.6, Typical MSBR Compositions and Properties, Figure 13.31, MSBR Fuel Processing Flow Diagram, *Basic Nuclear Engineering, 2nd Ed.* (Allyn and Bacon, Incorporated, Boston, MA, 1973) pp. 72-80, 330-342, 416-422, 446-449.

Kazuo Furukawa and Hideo Ohno, "Databook for molten materials: 1 – Molten LiF-BeF_2 (FLIBE)", published by the Society of Molten-Salt Thermal Technology, Japan Nuclear-Energy Information Center (1980). (123 pages).

Victor Ignatiev, Aleksander Merzlyakov, Vladimir Gorbunov, Valery Afonichkin, Vladimir Khokhlov, Aleksander Salyulev, Yuri Golovatov, Konstantin Grebenkine, Aleksander Panov, and Vladimir Subbotin, "Physical and Chemical Properties of Molten Salt Reactor Fuel Salts" Proceedings of ICAPP'03, Cordoba Spain, May 4-7, 2003, Paper 3030 (10 Pages).

V. Ignatiev, V. Gorbunov, R. Zakirov. Fuels and fission products clean up for molten salt reactor of the incinerator type. ATALANTE 2004: Advances for future nuclear fuel cycles. Nimes, France June 21-14, 2004.

V.V. Ignatiev, A. Merzlyakov, V.G. Subbotin, A.V. Panov, and Yu. V. Golovatov, Experimental investigation of the physical properties of salt melts containing sodium and lithium fluorides and beryllium difluoride. Atomic Energy, 101 822-829 (2006).

International Atomic Energy Agency, "The Physical Protection of Nuclear Material and Nuclear Facilities," INFCIRC/225/Rev.4 http://www.iaea.org/worldatom/program/protection/index.html).

L. Kaufman, J. Agren, J. Nell, and F. Hayes, "Calculation of Ternary Fluoride Glass Compositions", CALPHAD 7, 71-83 (1983).

L. Kaufman and H. Bernstein, "Computer Calculation of Phase Diagrams with Special Reference to Refractory Metals" (Academic Press, New York, 1970a).

L. Kaufman and H. Bernstein, "Computer Calculations of Phase Diagrams" (Academic Press, New York, 1970b), p. 37-42.

J.-G. Kim, J.-H. Lee, E.-H. Kim, D.-H. Ahn, J.-H. Kim, Conditioning of waste LiCl salt from pyrchemical process using zeolite A. Proc. Waste Management 2006 Conf. Feb 26-Mar 2, 2006, Tucson, AZ.

O. Kubachewki and C. A. Alcock, "Metallurgical Thermochemistry" (Pergamon Press, Oxford, 1979), 5th edition, p. 364-374.

J. D. Lee, et al., "Feasibility Study of a Fission-Suppressed Tandem-Mirror Hybrid Reactor", Lawrence Livermore National Laboratory, Livermore, CA, UCID-19327 (1982).

http://moltensalt.org/references/static/ralphmoir/UCID19327pt1.pdf

http://moltensalt.org/references/static/ralphmoir/UCID19327pt2.pdf

http://moltensalt.org/references/static/ralphmoir/UCID19327ChapterVII.pdf

James C. Mailen, Fred J. Smith, and Leslie M. Ferris, "Solubility of PuF_3 in molten 2 LiF-BeF_2", J. of Chem. and Eng. Data **16** (1), 68-69 (1971).

Juliette van der Meer, "Thermochemical investigation of molten fluoride salts for Generation IV nuclear application – An equilibrium exercise", Thesis from the Faculty of Geosciences of the University of Utrecht No. 262 (ISBN 90-5744-126-8, 2006) (179 pages).

J. P. M. van der Meer, R. J. M. Konings, and H. A. J. Oonk, "Thermodynamic assessment of the LiF–BeF_2–ThF_4–UF_4 system", J. of Nucl. Mater. **357**, 48-57 (2006); and references therein.

A. P. Miodownik, "Phenomenological calculations of phase equilibria: the CALPHAD approach", in NATO-ASI Proceedings, Series B: Physics, Vol. **319**, eds. P. E. A. Turchi and A. Gonis (Plenum Press, NY, 1994), p. 45-79.

R. W. Moir, et al., "Design of a Helium-Cooled Molten Salt Fusion Breeder", *Fusion Technology*, Vol. 8, No. 1 Part 2(A) 465 (1985).

MRS Bulletin, Vol. **24**, No. 4 (April 1999), "*Computer Simulations from Thermodynamic Data: Materials Production and Development*", p. 18-49.

N.R. Mulford. Calculation of the LiF-CeF_3-BeF_2 and LiF-PuF-BeF_2 Ternary Phase Diagrams. Los Alamos National Laboratory LA-12569 (1993)

National Research Council, *Electrometallurgical Techniques for DOE Spent Fuel*

Treatment: Final Report. Committee on Electrometallurgical Techniques for DOE

Spent Fuel Treatment, National Research Council. National Academy Press, Washington, DC. 116 pp.

Olander, D.L., Redox condition in molten fluoride salts: Definition and control. J. Nucl. Mat. 300:2-3 2002, pp270-272.

J. Powers, "Preliminary Neutronics Design Studies for a Molten Salt Blanket LIFE Engine," (August 6, 2008).

O. Redlich and A. Kister, "Algebraic Representation of the Thermodynamic Properties and the Classification of Solutions", Ind. Eng. Chem. **40**, 345-348 (1948).

M. W. Rosenthal, P. R. Kasten, R. B. Briggs: Nuclear Technology 8, 2 (1970) 111.

M.W. Rosenthal, P.N. Haubenreich, R.B. Briggs, The Development Status of Molten Salt Reactors. ORNL-4812 (1972).

N. Saunders and A. P. Miodownik, "*CALPHAD, Calculation of Phase Diagrams: A Comprehensive Guide*", Pergamon Materials Series, vol. 1, ed. by R W. Cahn (Pergamon Press, Oxford, 1998).

Peter Song, private communication (June 2008).

The Thermo-Calc application software are products of Thermo-Calc AB; B. Sundman, B. Jansson, and J.O. Andersson, "The Thermo-Calc Databank System", CALPHAD **9** (4), 153 (1985); J.O. Andersson, T. Helander, L. Höglund, Pingfang Shi, and B. Sundman, "THERMO-CALC & DICTRA, computational tools for materials science", CALPHAD **26** (2), 273-312 (2002); cf. also http://www.thermocalc.se.

R. E. Thoma, "Phase diagrams of nuclear reactors", ORNL-2548 (November 1959) (213 pages).

M.E. Whatley, L.E. McNeese, W.L. Carter, L.M. Ferris, E.L. Nicholson, Engineering Development of the MSBR Fuel Recyle. Nucl. Appl. Tech. 8, 170-178 (1970).

D. F. Williams, L. M. Toth, and K. T. Clarno, "Assessment of candidate salt coolants for the advanced high-temperature reactor (AHTR)", ORNL/TM2006/12 (March 2006). (86 pages).

Appendix A– Calculation of the Vapor Pressure over Solutions

From classical thermodynamics, the Gibbs free energy for a binary solution $A_{1-x}B_x$ in the liquid phase (in the following, L will stand for Liquid) can be expressed as follows (Kaufman and Bernstein, 1970b):

$$G^L = (1-x)^0 G_A^L + x^0 G_B^L + RT\left[x\ln x + (1-x)\ln(1-x)\right] + {}^{xs}G^L$$

where ${}^0G_i^L$ is the Gibbs energy of component i (i =A, B) in the L phase, the third term is the ideal mixing entropy term (with R and T being the gas constant and the temperature, respectively), and the last term is the excess Gibbs energy of mixing that can be expressed as:

$${}^{xs}G^L = x(1-x)\sum_{k=0,p} {}^kL_{A,B}^L (1-2x)^k$$

where ${}^kL_{A,B}^L$ is the k[th]-order binary interaction parameter between A and B expressed as a polynomial in temperature T in a so-called Redlich-Kister expansion of the excess Gibbs energy (Radlich and Kister, 1948). Note that when all the L parameters are set to zero, we have the ideal solution approximation, and if only ${}^0L_{A,B}^L \neq 0$ (all the other interactions associated with k>0 are set to zero), then we have the regular solution approximation. From this expression for the total Gibbs energy it is simple to derive the partial Gibbs energies given by:

$$G_A^L = G^L - x\frac{\partial G^L}{\partial x} \text{ and } G_B^L = G^L + (1-x)\frac{\partial G^L}{\partial x}$$

that become, with the expression for the total Gibbs energy:

$$G_A^L = {}^0G_A^L + RT\ln(1-x) + x^2\sum_{k=0,p} {}^kL_{A,B}^L (1-2x)^k + 2x^2(1-x)\sum_{k=1,p} k\ {}^kL_{A,B}^L (1-2x)^{k-1}$$

with a similar expression for G_B^L (where x and $1-x$ have been permuted). For ideal gases, the partial pressure is given by the following expression:

$$RT\ln\frac{p_i^L}{p_i^0} = RT\ln\frac{a_i^L}{a_i^0}$$

where a_i^L and a_i^0 are the activities of component i in the L phase and the pure phase, respectively, then we have

$$RT\ln\frac{p_i^L}{p_i^0} = \Delta G_i^{0\to L} + RT\ln(1-x) + x^2\sum_{k=0,p} {}^kL_{A,B}^L (1-2x)^k + 2x^2(1-x)\sum_{k=1,p} k\ {}^kL_{A,B}^L (1-2x)^{k-1}$$

Note that in the case of a regular solution model (model that will be considered in the following) with ${}^{0}L_{A,B}^{L} = \Omega$, the partial vapor pressures of A and B associated with the solution $A-B$ are simply given by:

$$p_A = p_A^0 \exp\left[\ln(x_A) + \frac{x_B^2}{RT}\Omega\right] \text{ and } p_B = p_B^0 \exp\left[\ln(x_B) + \frac{x_A^2}{RT}\Omega\right]$$

where p_i^0 is the vapor pressure associated with the pure component i.

Appendix B Summary of published data on the modeling of the thermodynamic properties of salts.

References	Binaries	Ternaries	Quaternaries
J. of Nucl. Mater. **377**, 449-457 (2008) "Actinide Burner Fuel: Potential compositions based on the thermodynamic evaluation of MF-PuF_3 (M=Li, Na, K, Rb, Cs) and LaF_3-PuF_3 systems", O. Benes and R.J.M. Konings	KF-PuF_3 RbF-PuF_3 CsF-PuF_3 LaF_3-PuF_3	LiF-NaF-PuF_3 LiF-CsF-PuF_3 LiF-KF-PuF_3 LiF-LaF_3-PuF_3 LiF-RbF-PuF_3 NaF-KF-PuF_3 NaF-RbF-PuF_3 KF-RbF-PuF_3 NaF-CsF-PuF_3 KF-CsF-PuF_3 NaF-LaF_3-PuF_3 KF-LaF_3-PuF_3 RbF-CF-PuF_3 RbF-LaF_3-PuF_3 CsF-LaF_3-PuF_3	LiF-KF-RbF-PuF_3 LiF-NaF-KF-PuF_3 LiF-NaF-RbF-PuF_3
CALPHAD **32**, 121-128 (2008) "Thermodynamic evaluation of the MF–LaF_3 (M = Li, Na, K, Rb, Cs) systems", O. Benes and R. J. M. Konings	KF-LaF_3 CsF-LaF_3	LiF-KF-LaF_3 LiF-CsF-LaF_3 NaF-KF-LaF_3 KF-RbF-LaF_3 NaF-CsF-LaF_3 KF-CsF-LaF_3 RbF-CsF-LaF_3	N/A
Preprint (2008), 40 pages "Modelling and calculation of the LiF-NaF-MF_3 (M=La, Ce, Pu) phase diagrams", J. P. M. van der Meer, R. J. M. Konings, K. Hack, and H. A. J. Oonk	LiF-NaF LiF-LaF_3 LiF-CeF_3 LiF-PuF_3 NaF-LaF_3 NaF-CeF_3 NaF-PuF_3	LiF-NaF-LaF_3 LiF-NaF-CeF_3 LiF-NaF-PuF_3	N/A
J. of Alloys and Cmpds **45**2, 110-115 (2008) "Thermodynamic study of LiF-BeF_2-ZrF_4-UF_4 system", O. Benes and R. J. M. Konings	LiF-ZrF_4 BeF_2-ZrF_4 UF4-ZrF_4	LiF-BeF_2-ZrF_4 LiF-BeF_2-UF_4 BeF_2-ZrF_4-UF_4	LiF-BeF_2-ZrF_4-UF_4
J. of Nucl. Mater. **360**, 16-24 (2007)	N/A	LiF–BeF_2–ThF_4	N/A

"Thermal and physical properties of molten fluorides for nuclear applications", J.P.M. van der Meer and R.J.M. Konings			
CALPHAD **31**, 209-216 (2007) "Modelling and calculation of the phase diagrams of the LiF–NaF–$RbF–LaF_3$ system", O. Benes, J. P. M. van der Meer, and R. J. M. Konings	LiF-NaF LiF-RbF NaF-RbF $RbF-LaF_3$	LiF-NaF-RbF $LiF-RbF-LaF_3$ $NaF-RbF-LaF_3$ $LiF-NaF-LaF_3$	LiF–NaF–RbF–LaF_3
J. of Nucl. Mater. **357**, 48-57 (2006) "Thermodynamic assessment of the $LiF–BeF_2–ThF_4–UF_4$ system", J. P. M. van der Meer, R. J. M. Konings, and H. A. J. Oonk	$LiF-UF_4$ $LiF-ThF_4$ BeF_2-UF_4 ThF_4-UF_4	$LiF–BeF_2–ThF_4$ $LiF–BeF_2–UF_4$ $LiF–ThF_4–UF_4$ $BeF_2–ThF_4–UF_4$	$LiF–BeF_2–ThF_4–UF_4$
J. of Nucl. Mater. **344**, 94-99 (2005) "A miscibility gap in $LiF–BeF_2$ and $LiF–BeF_2–ThF_4$", J. P. M. van der Meer, R. J. M. Konings, M. H. G. Jacobs, and H. A. J. Oonk	$LiF–BeF_2$ $LiF–ThF_4$ $BeF_2–ThF_4$	$LiF–BeF_2–ThF_4$	N/A
Chem. Mater. **18**, 510-517 (2006) "Modeling and calculation of the $LiF-NaF-MF_3$ (M=La,Ce,Pu) phase diagram", J. P. M. van der Meer, R. J. M. Konings, K. Hack, and H. A. J. Oonk	LiF-NaF $LiF-LaF_3$ $LiF-CeF_3$ $LiF-PuF_3$ $NaF-LaF_3$ $NaF-CeF_3$ $NaF-PuF_3$	$LiF-NaF-LaF_3$ $LiF-NaF-CeF_3$ $LiF-NaF-PuF_3$	N/A
J. of Nucl. Mater. **335**, 345-352 (2004) "Thermodynamic modelling of $LiF–LnF_3$ and $LiF–AnF_3$ phase diagrams", J.P.M. van der Meer, R.J.M. Konings, M.H.G. Jacobs, and H.A.J. Oonk	$LiF–LaF_3$ $LiF–CeF_3$ $LiF–PrF_3$ $LiF–SmF_3$ $LiF–NdF_3$ $LiF–PuF_3$ $LiF–UF_3$ $LiF-AmF_3$	$LiF–PuF_3-AmF_3$	N/A
J. of Nucl. Mater. **375**, 202-208 (2008) "Thermodynamic evaluation of the $NaCl-MgCl_2-UCl_3-PuCl_3$ system", O. Benes, and R.J.M. Konings	UCl_3-PuCl_3	$NaCl-MgCl_2-UCl_3$ $NaCl-MgCl_2-PuCl_3$ $NaCl-UCl_3-PuCl_3$	N/A

		$MgCl_2$-UCl_3-$PuCl_3$	
J. of Nucl. Mater. **344**, 173-179 (2005) "Thermochemical properties of lanthanides (Ln = La, Nd) and actinides (An = U, Np, Pu, Am) in the molten LiCl–KCl eutectic", Patrick Masset, Rudy J.M. Konings, Rikard Malmbeck, Jérôme Serp, and Jean-Paul Glatz	N/A	N/A	N/A

Tables

Table 1. Temperature at key points in the molten salt loop.

$T_{structure\ hot}$	720 to 750 °C
T_{out}	720
T_{in}	670
T_{cold}	640
T_{melt}	610

Table 2. Fluoride-forming fission products

Mol% based on G70 with REE removed which is RM2 (Powers, 2008).

Salt	**T_{melt}, °C**	**Peak mol% in melt**
Base salt components		
LiF	845	82.7
BeF_2	555	0
Actinides		
UF_3	>1000	
UF_4	960	
ThF_4	1111	
PuF_3	1425	2.3
NpF_3		0.05
AmF_3	1395	0.12
CmF_3		0.18
Alkalis and alkaline earths		
RbF	795	0.66

CsF	682	1.66
BaF_2	1355	6.0
SrF_2	1473	1.5
Rare earths		
YF_3	1387	0.83
LaF_3		
CeF_3	1460	
PrF_2		
NdF_3	1410	
PmF_3		
SmF_2	1306	
EuF_2	1380	
GdF_3		
TbF_3	1172	
DyF_3	1360	
HoF_3	1143	
ErF_3	1350	
TmF_3	1158	Not in data base
YbF_3	1052	Not in data base
Other species		
ZrF_4	~600 sublimes	6.5
TeF_2		0.88
AsF_3	?	Not in data base
SeF_2		0.17

Table 3. Ranking of nuclear properties for candidate salt constituents (Williams, Toth and Clarno, 2006).

	Moderating ratio	Short-lived activation	Long-lived activation
Lithium	Good	Very good	Very good
Beryllium	Very good	Very good	Good
Fluorine	Very good	Very good	Very good
Sodium	Acceptable	Acceptable	Good
Potassium	Poor	Acceptable	Poor
Rubidium	Acceptable	Poor	Good
Zirconium	Good	Poor	Acceptable

Table 4. Physical properties of selected molten-salt solvents (Williams, Toth and Clarno, 2006).

salt /mole %	at. wt /g·mol^{-1}	T_{fus} /K	ρ /kg·m^{-3}; T/K	C_p [a] /J·g^{-1}·K^{-1}	η /10^{-3} Pa·s	k /W·m^{-1}·K^{-1}
$LiF-BeF_2$ (66-34)	33.1	731	2413-0.4884*T	2.38	0.116 exp(3755/T)	1.1
$LiF-NaF-BeF_2$ (32-31-37)	38.7	588	2000 [a]	2.05	5 [a]	0.97
$NaF-BeF_2$ (57-43)	44.1	633	2371-0.37*T	2.18	0.034 exp(5164/T)	~ 1
LiF-NaF (61-39)	32.2	922	1985 [a]	~ 2.1	*unknown*	~ 0.9
LiF-NaF-KF (11.5-46.5-42)	41.2	727	2729-0.73*T	1.88	0.04 exp(4170/T)	0.6-1
LiF-RbF (43-57)	70.7	748	3488-0.69*T	1.19	0.021 exp(4678/T)	~ 6
$NaF-ZrF_4$ (50-50)	104.6	783	4044-0.93*T	1.17	0.071 exp(4168/T)	~ 1
$NaF-KF-ZrF_4$ (10-48-42)	102.3	658	3693-0.89*T	1.09	0.061 exp(3171/T)	~ 1
$LiF-NaF-ZrF_4$ (10-48-42)	71.56	733	3597-0.83*T	1.46	0.0685 exp(4647/T)	~ 1

[a] Valid at T=973 K

Table 5. Melting point of various fluoride salts.

Compound	$T_{Melting}$, °C
ThF_4	1111
UF_4	960
NpF_3	?
PuF_3	1425
AmF_3	~1395
CmF_3	N/A
BkF_3	N/A
CfF_3	N/A

Table 6. Solubility of PuF_3 (in mole %) in the salt $2LiF\text{-}BF_2$ (Mailen et al., 1971 and Ignatiev et al., 2003).

Mailen			Ignatiev		
T (^{o}C)	Time (hr)	Solubility	T (^{o}C)	Time (hr)	Solubility
522	6	0.23	525	20	0.35
574	6	0.39	575	25	0.52
625	6	0.67	625	27	0.76
657	19	0.72	675	32	1.22

Table 7. Potential compositions of Pu-containing fluoride salts with melting temperature, vapor pressure (at 988 K), and boiling temperature. As an example, the range of existence of a liquid phase at 823 K in the case of $LiF\text{-}NaF\text{-}BeF_2$, with 1.3 mole% PuF_3 is shown (cf. Fig 29).

Composition mole %	$T_{Melting}$ K	P_{vapor} Pa at 988 K	$T_{Boiling}$ K
$LiF\text{-}NaF\text{-}PuF_3$ .580-.407-.013	917	N/A	N/A
$NaF\text{-}BeF_2\text{-}PuF_3$ .710-.277-.013	837	N/A	N/A
LiF-NaF-BeF2-PuF3 .203-.571-.212-.013	T_{inlet}: 873 T_{outlet}: 988	.001 .046	1973
$LiF\text{-}KF\text{-}PuF_3$ .482-.505-.013	760	0.8	1917
$LiF\text{-}RbF\text{-}PuF_3$ .439-.548-.013	744	3.5	1839
$LiF\text{-}NaF\text{-}RbF\text{-}PuF_3$ .395-.140-.452-.013	706	3.2	1926
$LiF\text{-}NaF\text{-}KF\text{-}PuF_3$ .433-.140-.414-.013	723	0.7	1937
$LiF\text{-}KF\text{-}RbF\text{-}PuF_3$ .428-.188-.371-.013	711	2.8	1863

Table 8. Blanket and Coolant Properties from references (Williams, Toth and Clarno, 2006, Moir, 1985, Foster and Wright, 1973 and Rosenthal, Kasten and Briggs, 1970).

Salt Formula	Formula Weight	Melting Point	Latent Heat of Fusion	Vapor Pressure (900°C)	Density	Heat Capacity (700°C)	Viscosity	Thermal Conductivity	Neutron Capture vs. Graphite	Moderating Ratio
	FW	MP	ΔH_f	P_{vap}	ρ	ρ □C_p	μ	K		
	(g/mol)	(ºC)	(cal/g)	(mm Hg)	(g/cm^3)	(cal/cm^3/º C)	(cP)	(W/m-K)		
Li	6.9	179			554					
Be	9.0	1283			1820					
Na	23.0	97.81			970					
K	39.1	63.65			860					
LiF	25.9	842			2300					
BeF_2	47.0				1086					
LiF-BeF_2	33.0	460		1.2	1.94	1.12	5.6	1.00	8	60
LiF-NaF-BeF_2	38.9	315		1.7	2.00	0.98	5.0	0.97	20	22
KF-ZrF_4	103.9	390		2.8	2.80	0.70	5.1	0.45	67	3
Rb-ZrF_4	132.9	410		1.3	3.22	0.64	5.1	0.39	14	13
LiF-NaF-ZrF_4	84.2	436		5 2	2.79	0.84	6.9	0.53	20	13
LiF-NaF-KF	41.3	454		0.7	2.02	0.91	2.9	0.92	90	2
LiF-NaF-RbF	67.7	435		0.8	2.69	0.63	2.6	0.62	20	8
72LiF-16BeF_2-12ThF_4			63.00	0.1 torr	3.35		12	1.10		
70LiF-12BeF_2-18ThF_4					3.87					
71LiF-2BeF_2-27ThF_4			54.00		4.52		15-25	0.70		

Table 9. In red are the binary combinations of fluoride salts that have been fully assessed and validated by available experimental data, and for which phase diagram information has been generated (as of August 2008).

	AmF_3	BeF_2	CeF_3	LaF_3	LiF	NaF	PuF_3	ThF_4	UF_4	ZrF_4
AmF_3										
BeF_2										
CeF_3										
LaF_3										
LiF										
NaF										
PuF_3										
ThF_4										
UF_4										
ZrF_4										

Table 10. Molten salt compositions considered for the calculation of the optimal fuel composition associated with minimum melting temperature.

LiF (mol%)	ThF_4 (mol%)	UF_4 (mol%)	PuF_3 (mol%)	Th/(Th+U)
76.0	24	0	0	1.000
76.5	21	3	.5	.875
75.0	18	6	1	.750
74.5	15	9	1.5	.625
74.25	13.5	10.5	1.75	.5625
74.0	12	12	2	.500
73.0	6	18	3	.250
72.0	0	24	4	.000

Table 11. Temperature at key points in the molten salt loop.

	Old estimate	New estimate
$T_{structure\ hot}$	720 to 750 °C	630 to 660
T_{out}	720	630
T_{in}	670	580
T_{cold}	640	550
T_{melt}	610	520

Figures

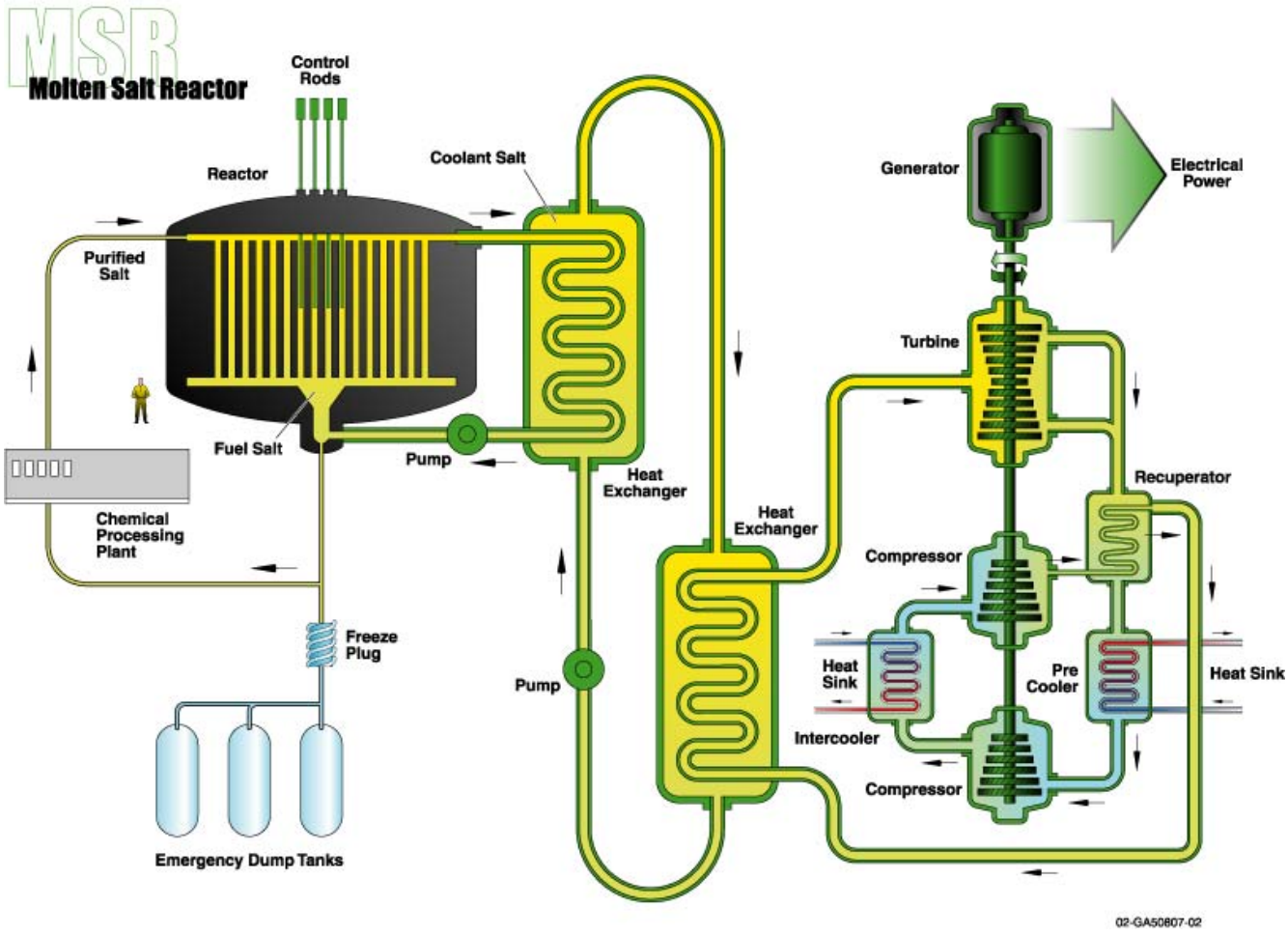

Figure 1. Generation IV Molten salt reactor concept [http://www.gen-4.org/Technology/systems/msr.htm].

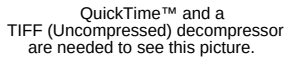

Figure 2a. Molten-Salt Reactor Experiment (MSRE) plant diagram.

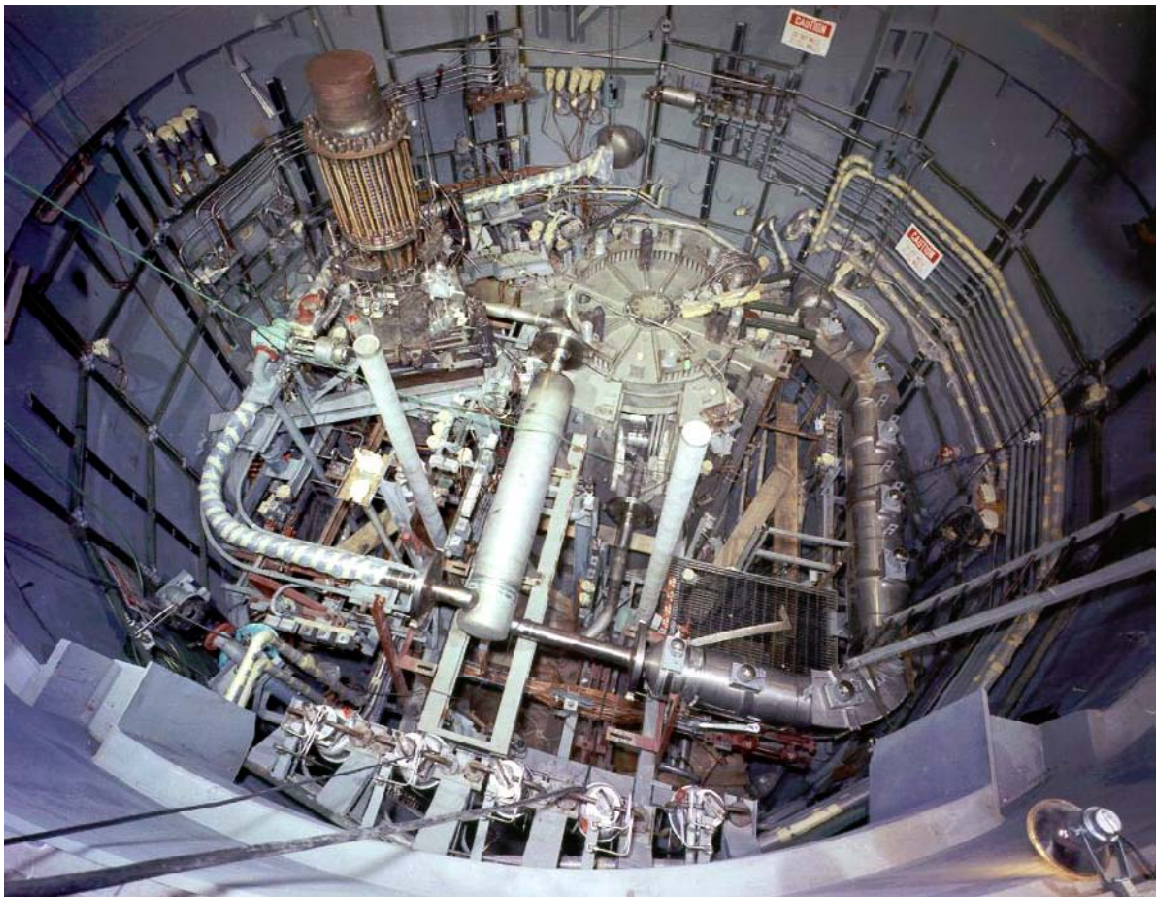

Figure 2b. Molten-Salt Reactor Experiment (MSRE)—inside containment vessel.

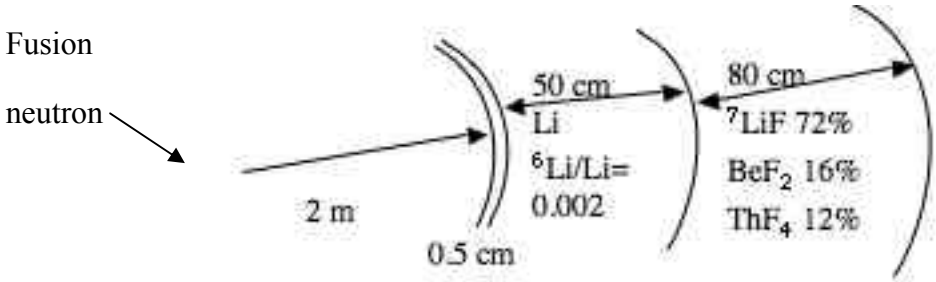

Figure 3. Molten salt blanket for a tandem mirror fusion breeder

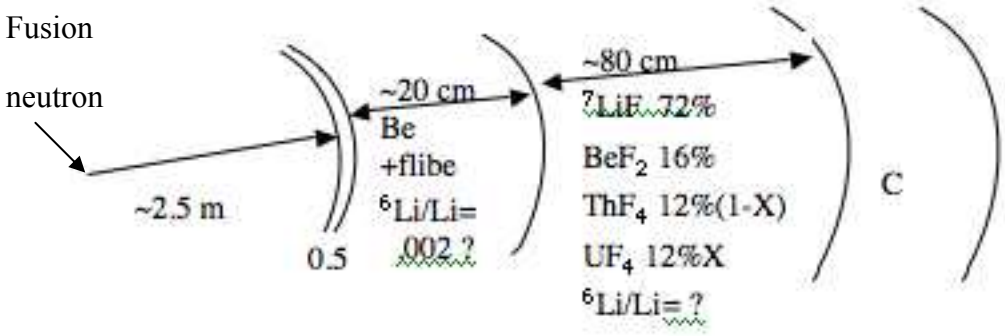

Figure 4. Molten salt blanket for LIFE

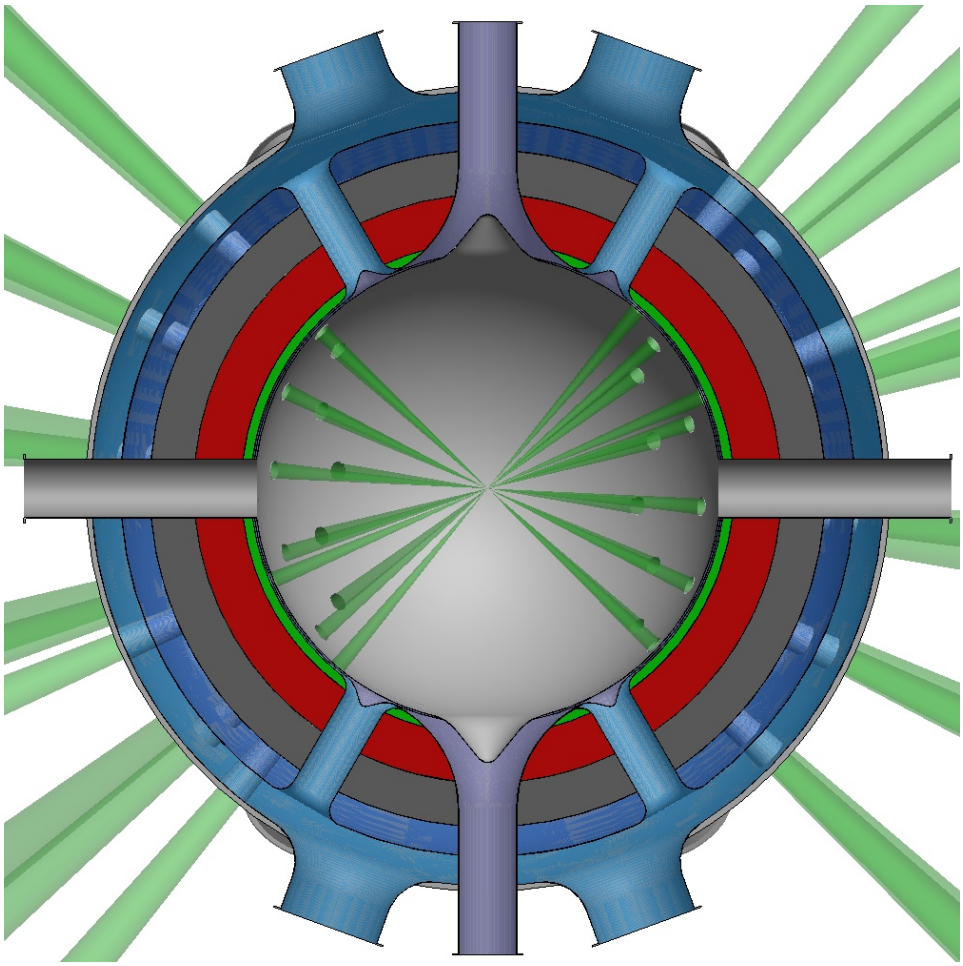

Figure 5. Molten salt blanket for the LIFE engine.

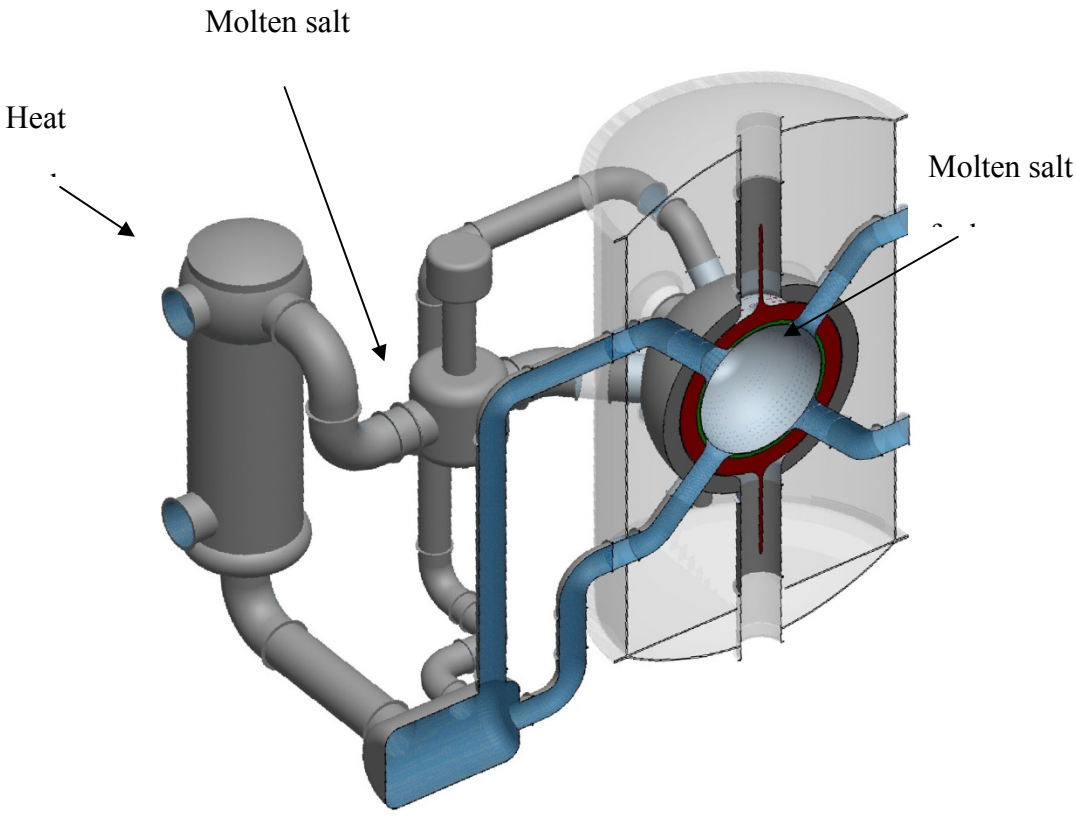

Figure 6. Illustration of LIFE blanket and flow loop.

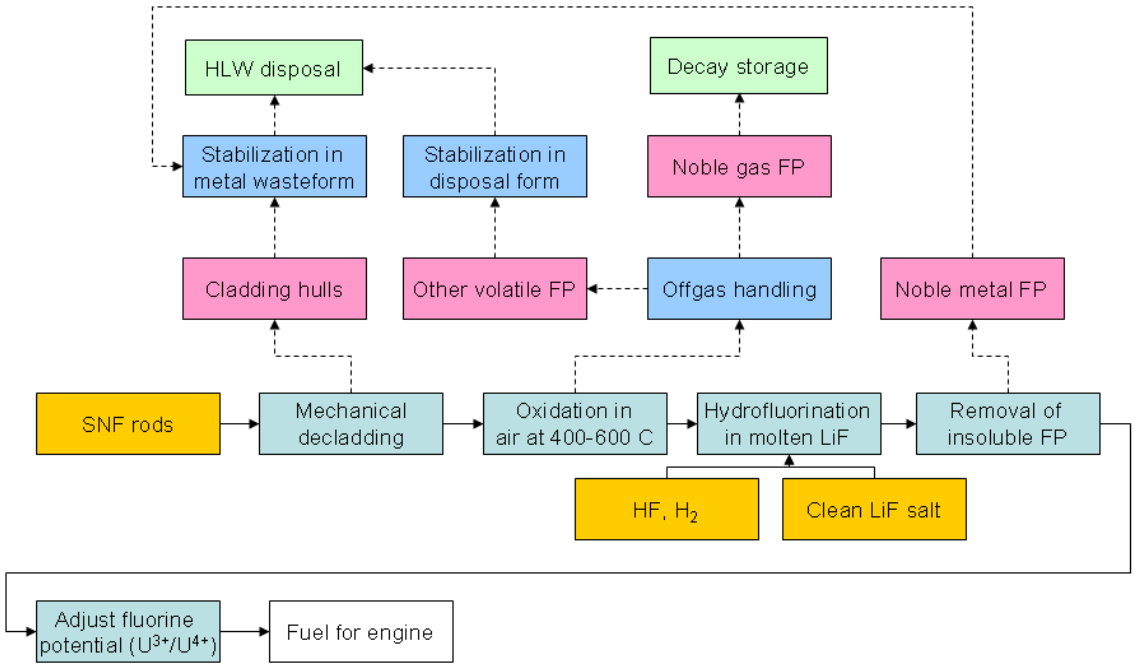

Figure 7. Process for converting LWR SNF into fuel for LIFE engine.

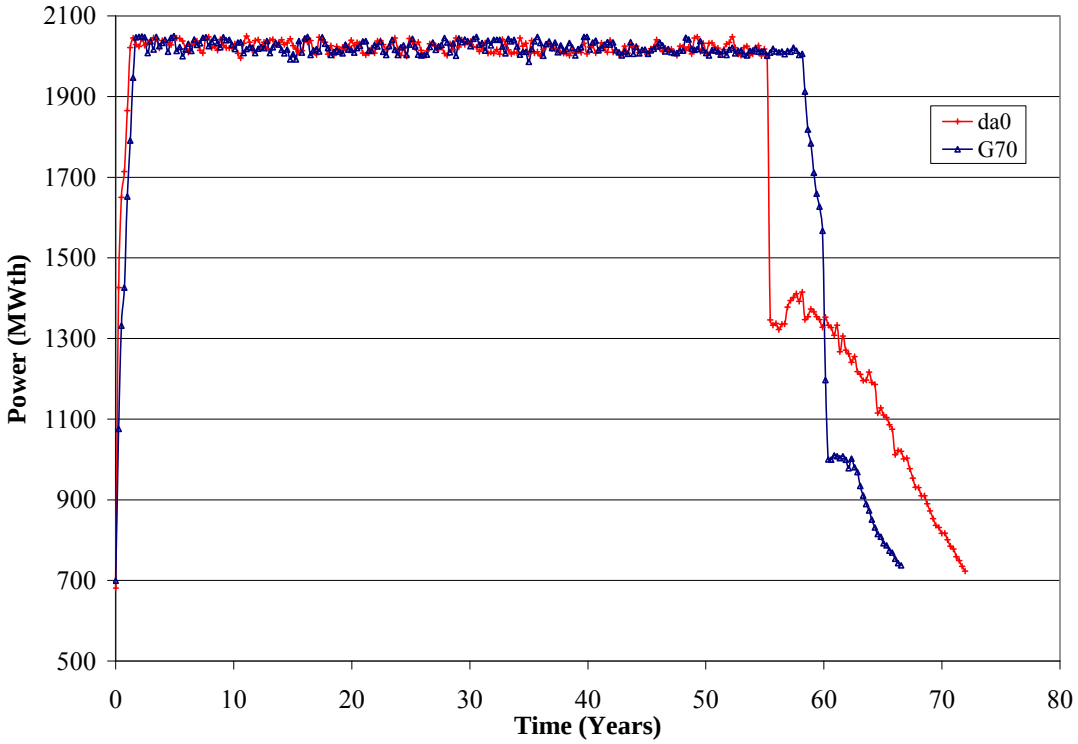

Figure 8. Power curves for cases G70 (molten salt) and da0 (TRISO fuel). (Fig 17 in Powers, 2008)

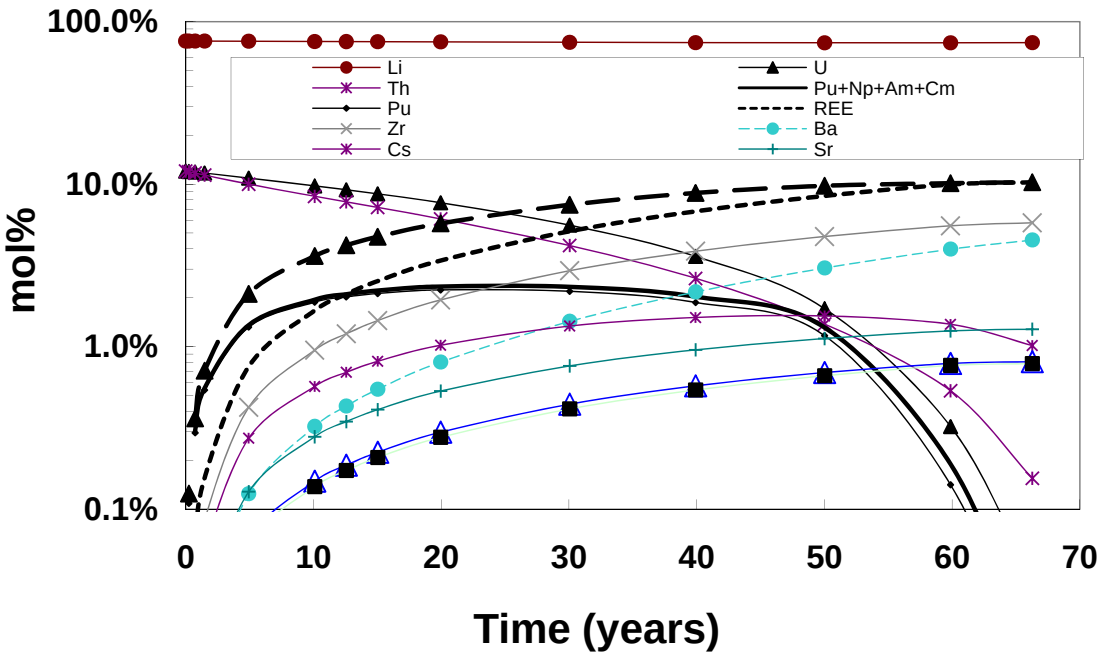

Figure 9. Evolution of the molten salt composition with time (case G70). Adapted from Figure 13 in Powers 2008.

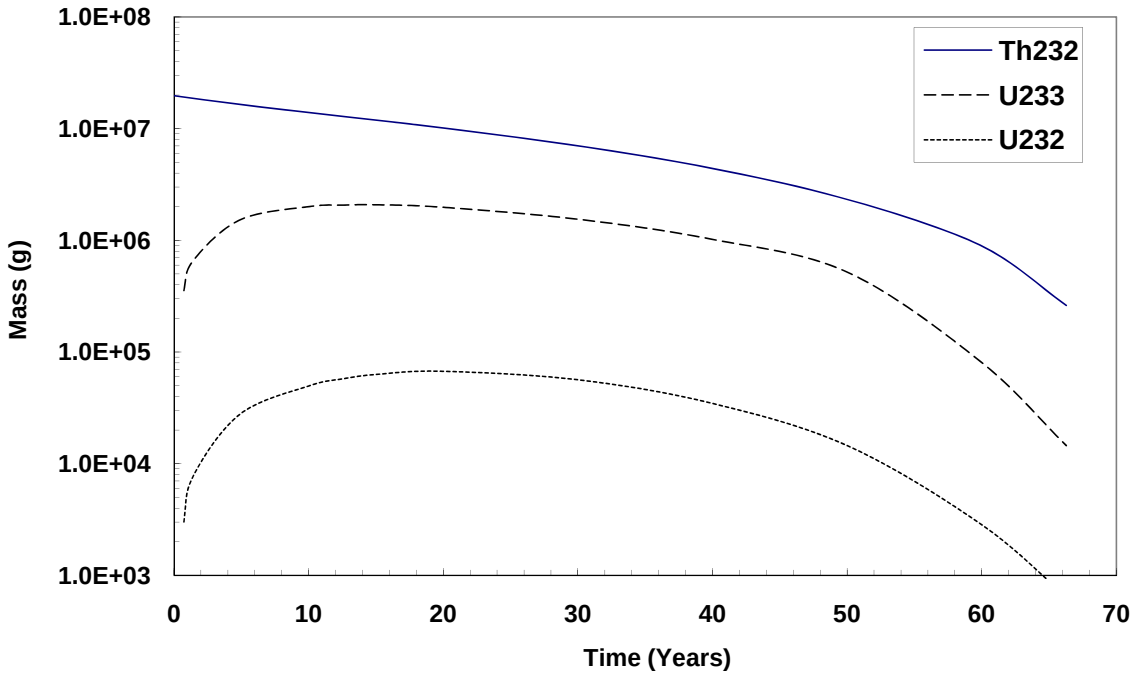

Figure 10. Time-dependent inventory of Th and U isotopes for Case G70.

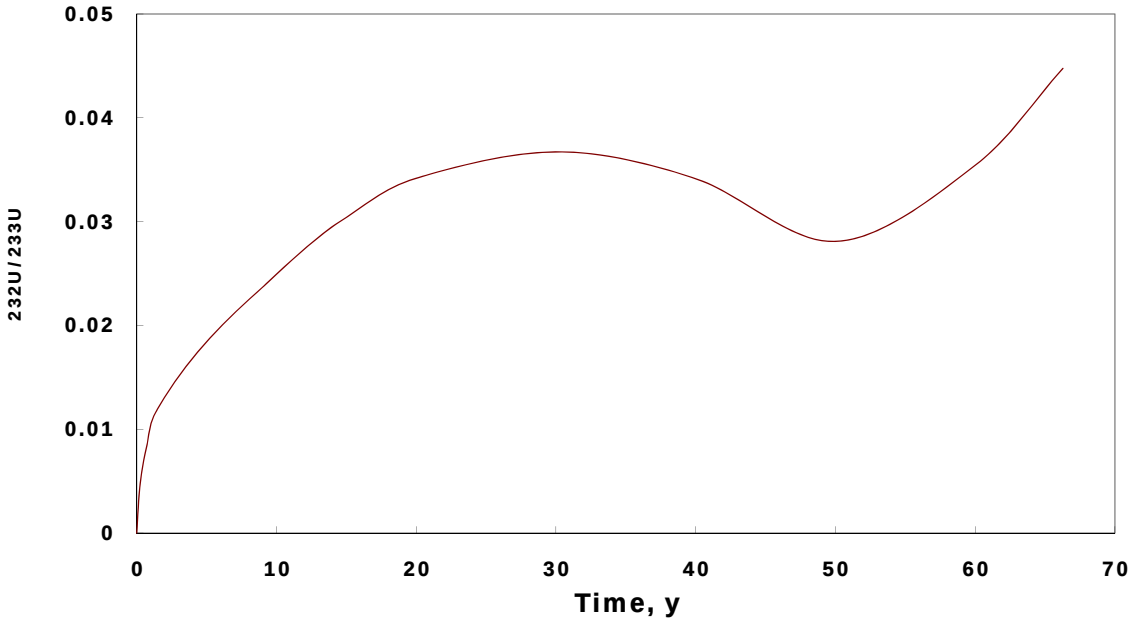

Figure 11. $^{232}U/^{233}U$ ratio versus burn time.

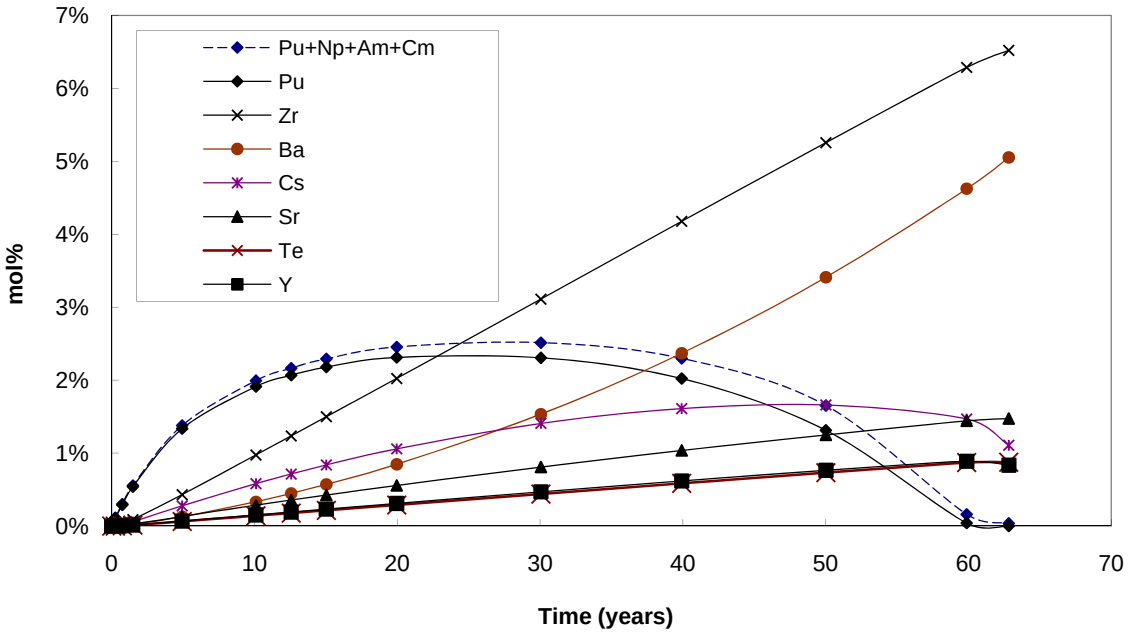

Figure 11. Evolution of for the molten salt composition with time for Case RM2 = G70 with REE removal. (Fig 28 in Powers, 2008)

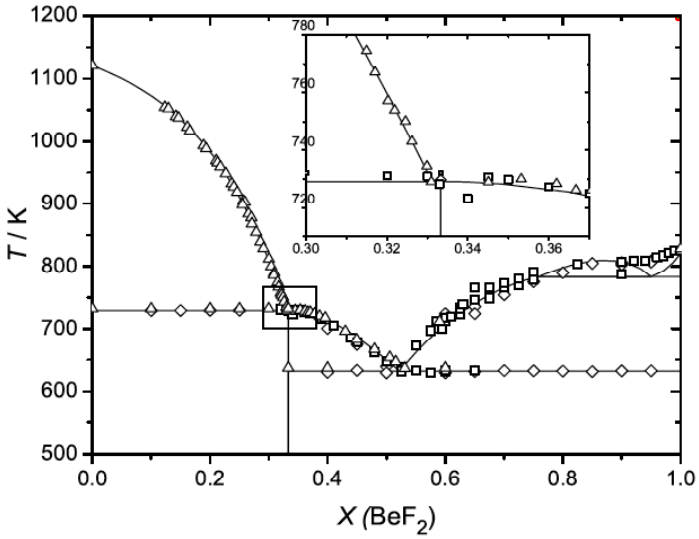

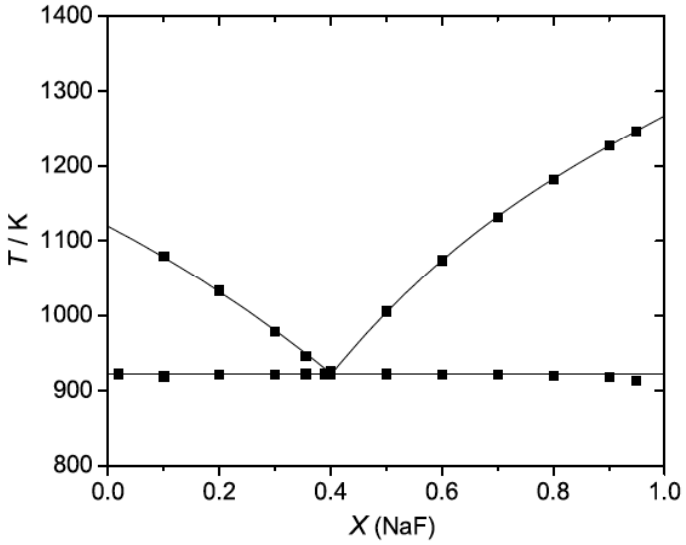

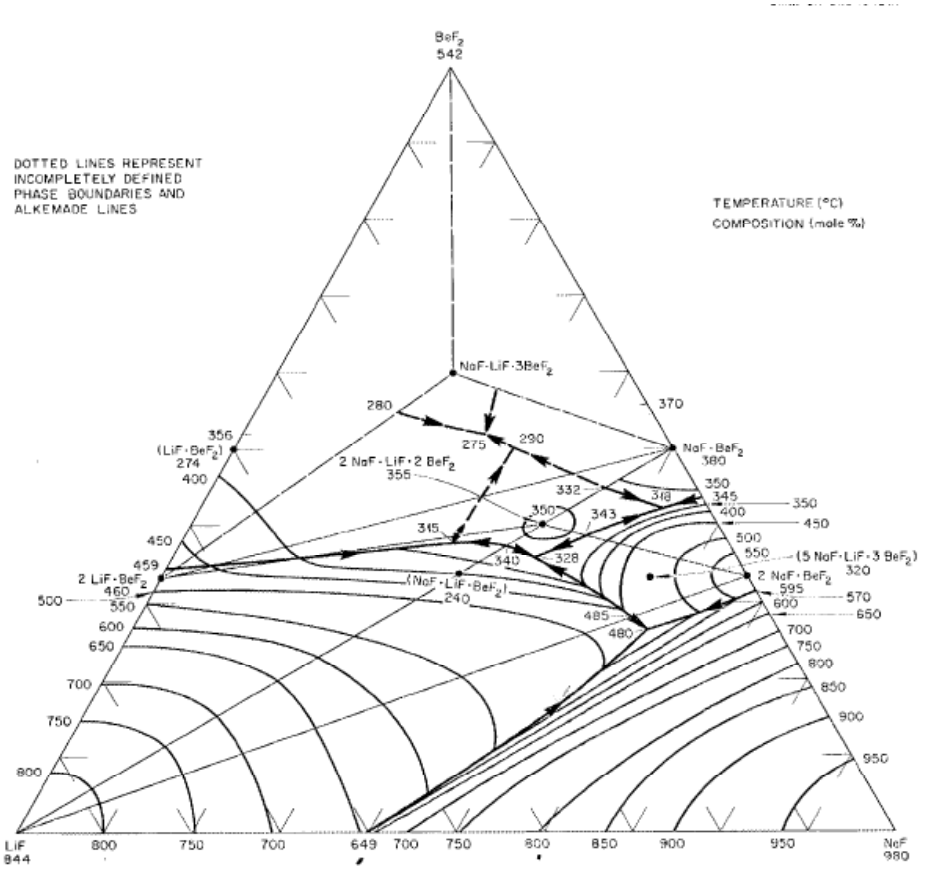

Figure 12. Phase diagrams of the binary LiF-BeF_2, LiF-NaF (Meer, 2006 and Thoma, 1959) and of the ternary LiF-NaF-BeF_2 salts (Thoma, 1959).

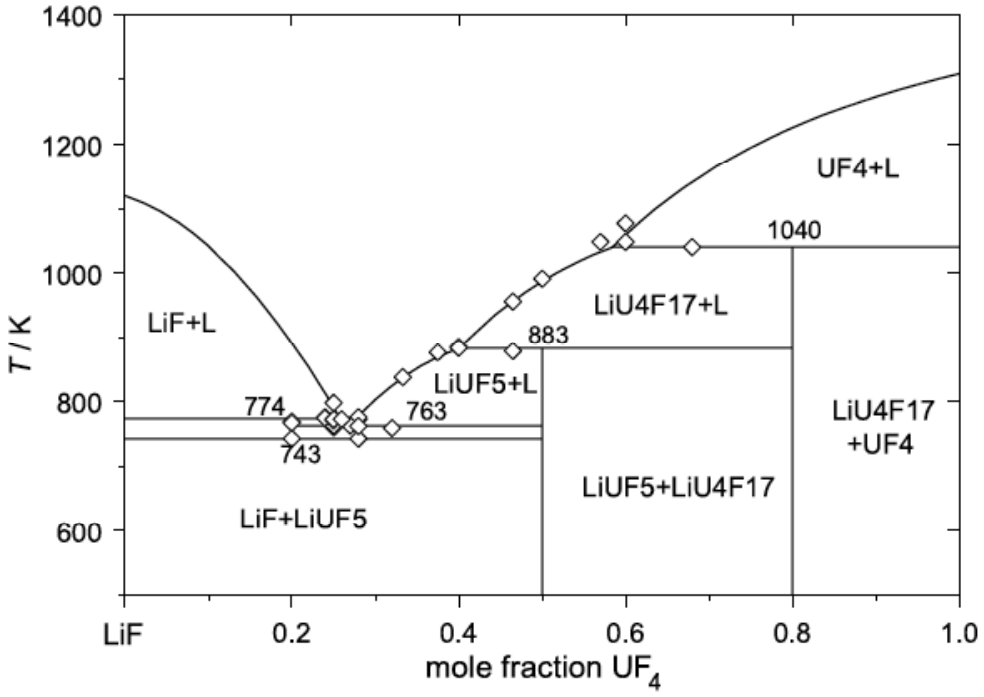

Figure 13. Phase diagram of the binary LiF-UF_4 salt (Meer, Konings and Oonk, 2006).

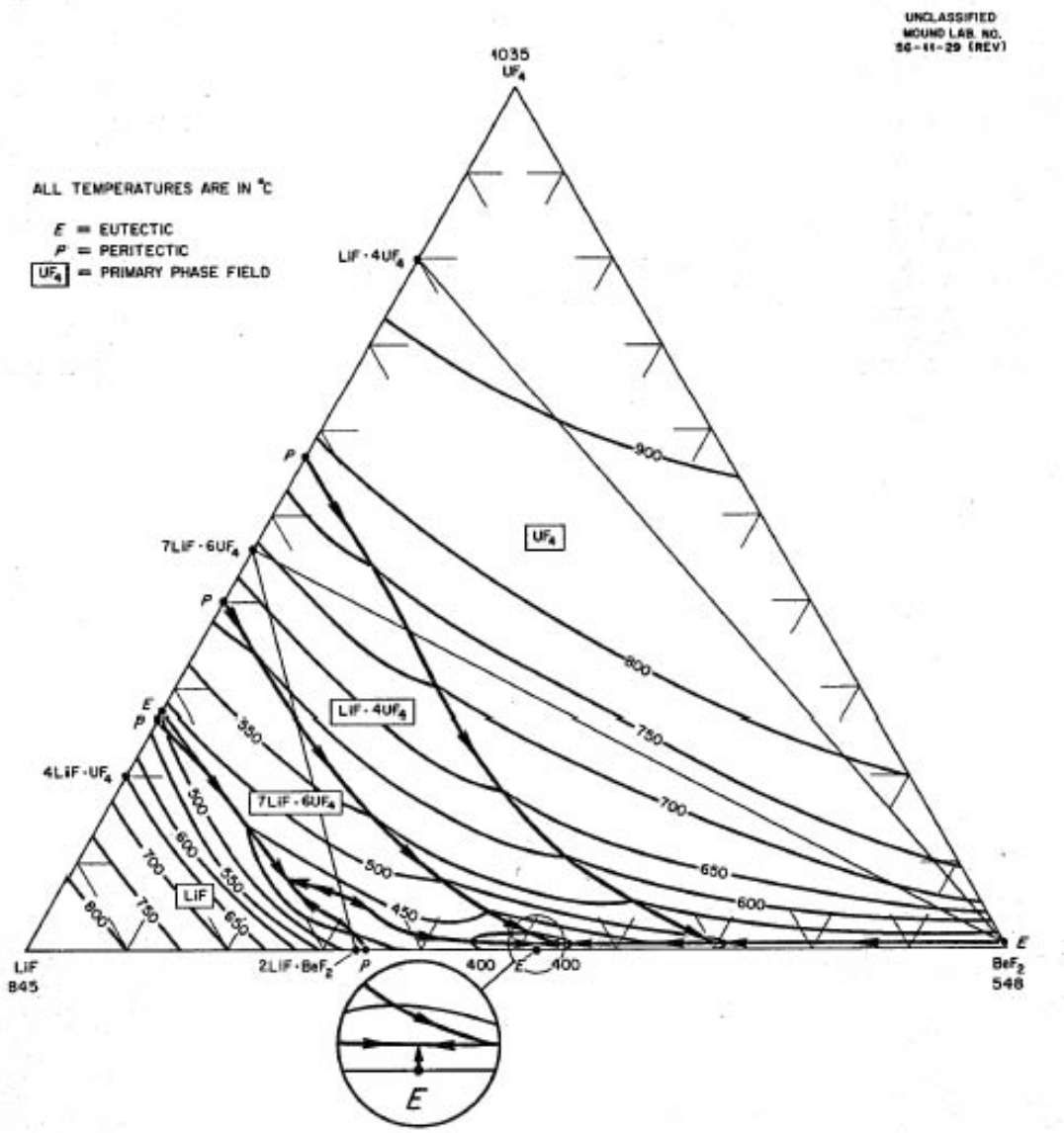

Fig. 3.69a. The System LiF–BeF_2–UF_4

Figure 14. Phase diagram of the ternary LiF-BeF2-UF_4 salt (Meer, Konings and Oonk, 2006).

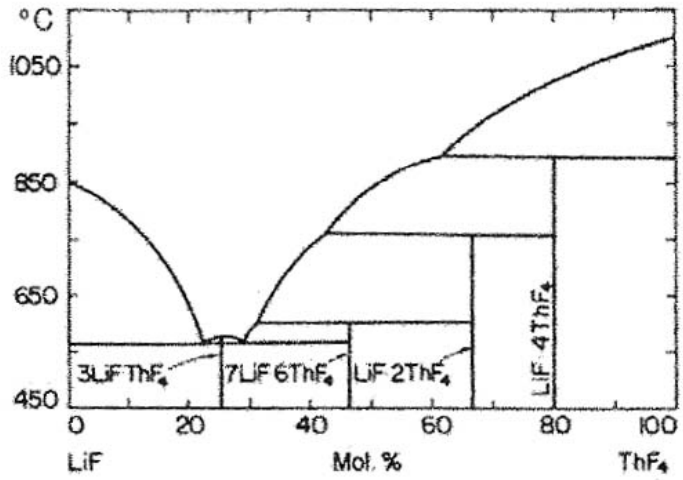

Figure 15. Phase diagram of the binary LiF-ThF_4 salt (Meer, Konings and Oonk, 2006).

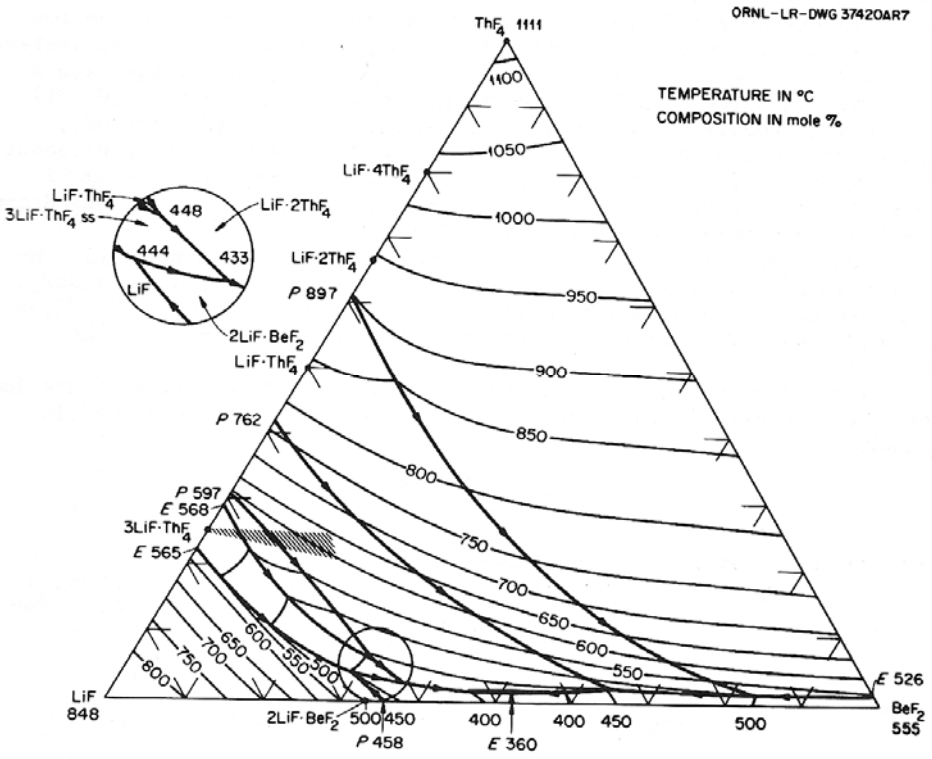

Figure 16. Phase diagram of the ternary LiF-BeF_2-ThF_4 salt (Meer, Konings and Oonk, 2006).

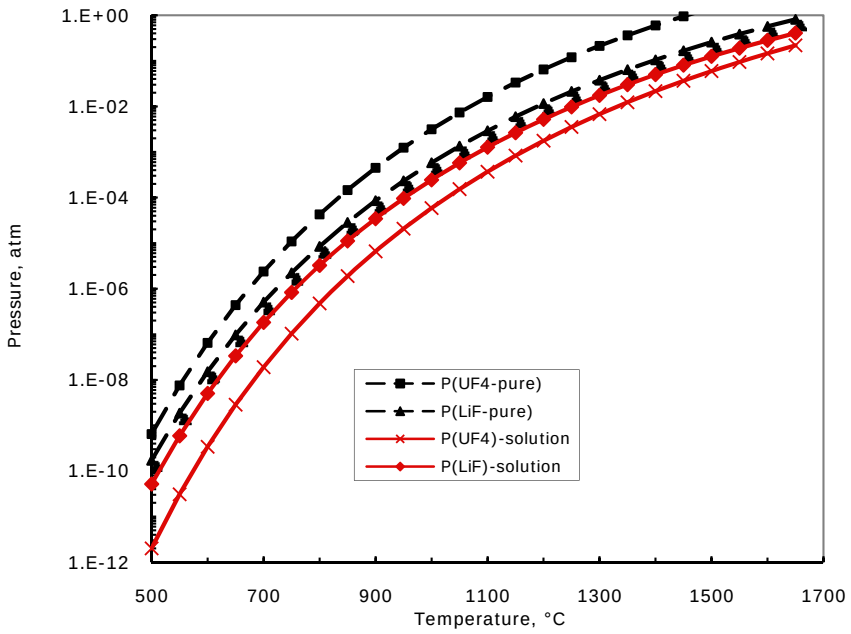

Figure 17. Vapor pressure of pure x_{UF_4} and x_{LiF} and over a solution with composition $x_{UF_4} = 0.3$ and $x_{LiF} = 0.7$.

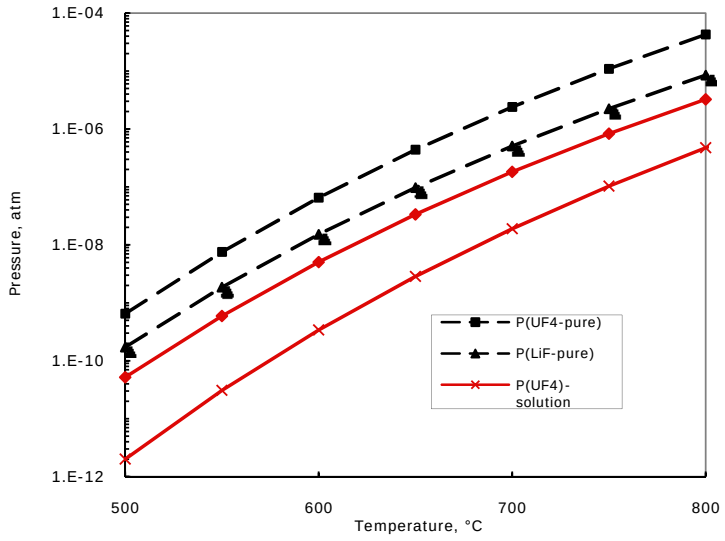

Figure 18. The same information shown in Fig. 17, over a smaller temperature range.

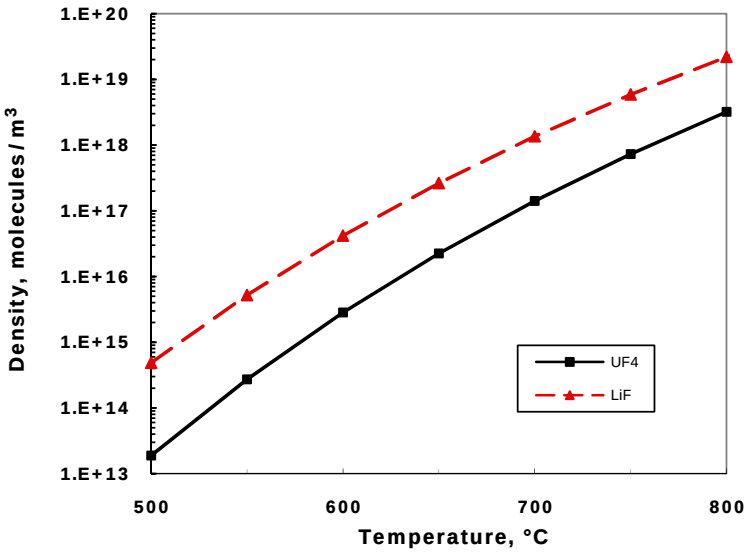

Figure 19. Vapor density for LiF (70%)-UF_4 (30%) versus temperature.

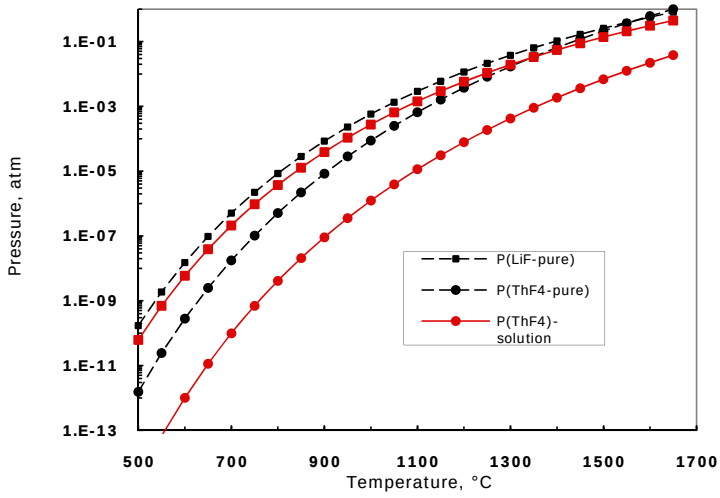

Figure 20. Vapor pressures over pure compounds and over (LiF) 0.725–(ThF_4) 0.275 versus temperature.

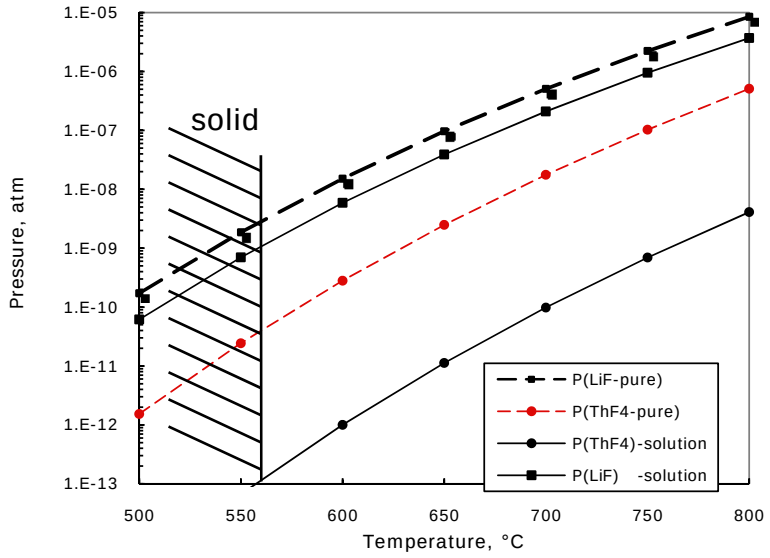

Figure 21. The same information as in Fig. 20 over a smaller temperature range.

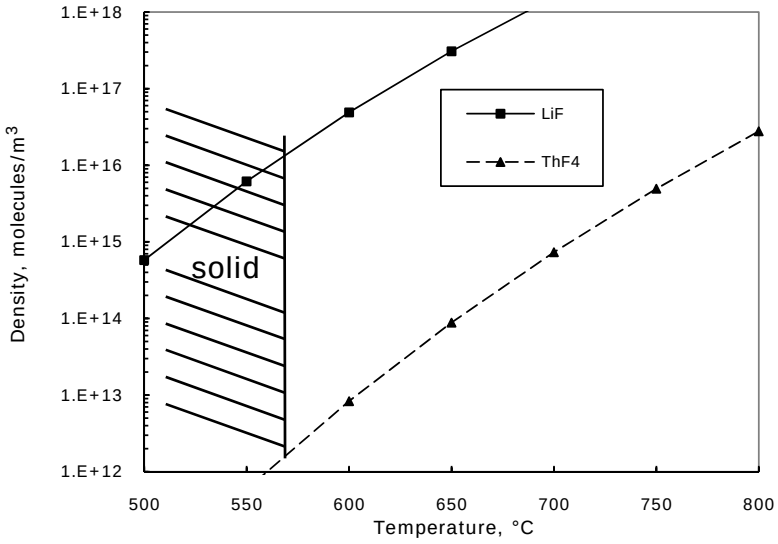

Figure 22. Vapor density for LiF-ThF_4 versus temperature.

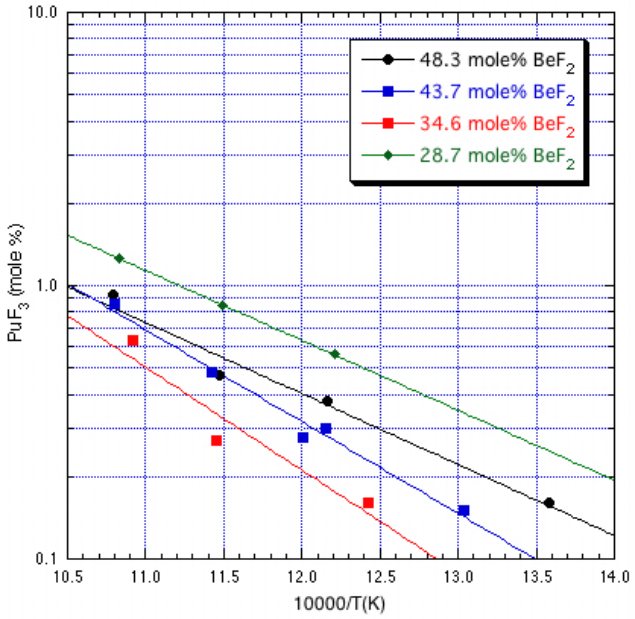

Figure 23. Original data on the solubility of PuF_3 in LiF-BeF_2 from Barton at T ≤ 654 °C (Barton and Strehlow, 1958, Barton, 1960 and Furukawa and Ohno, 1980).

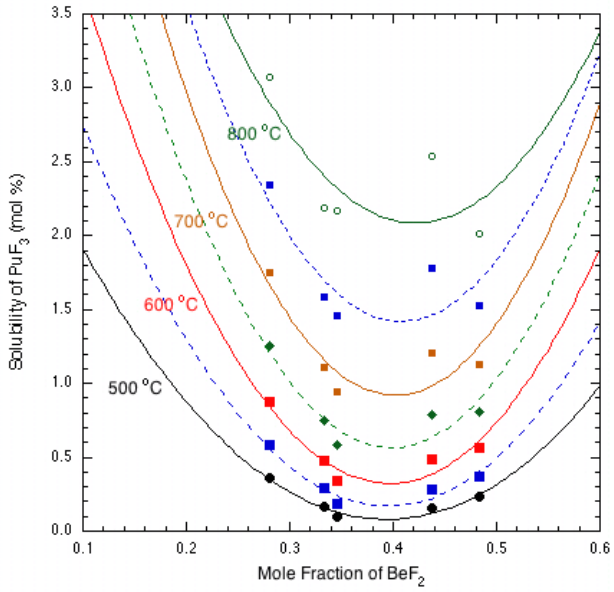

Figure 24. Barton's data on the solubility of PuF_3 in LiF-BeF_2 extrapolated up to 800 °C (Barton and Strehlow, 1958 and Barton, 1960).

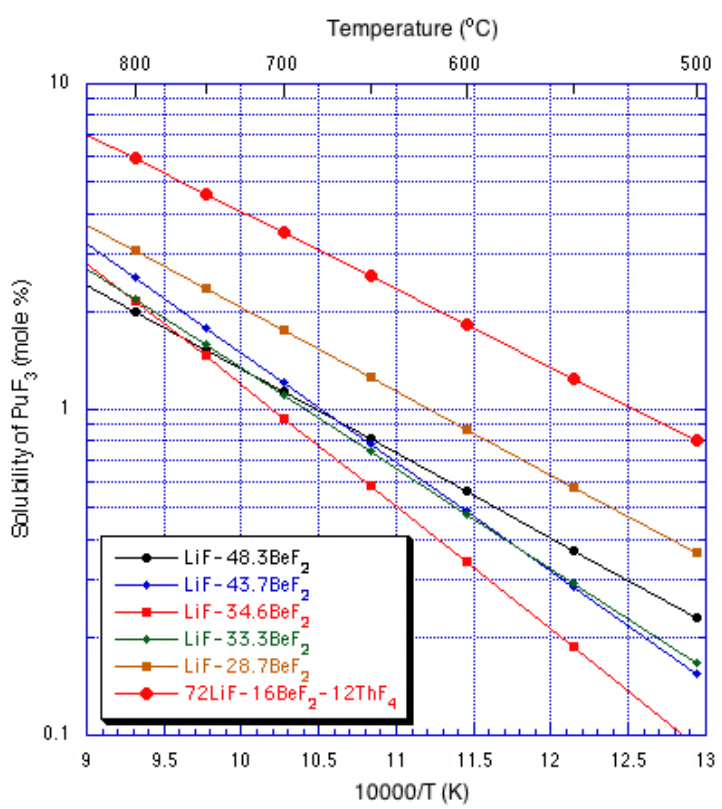

Figure 25. Summary of the results on the solubility of PuF_3 in LiF-BeF_2 of Barton and Strehlow, 1958, Mailen et al., 1971, and Bamberger et al., 1971 extrapolated up to 800 °C.

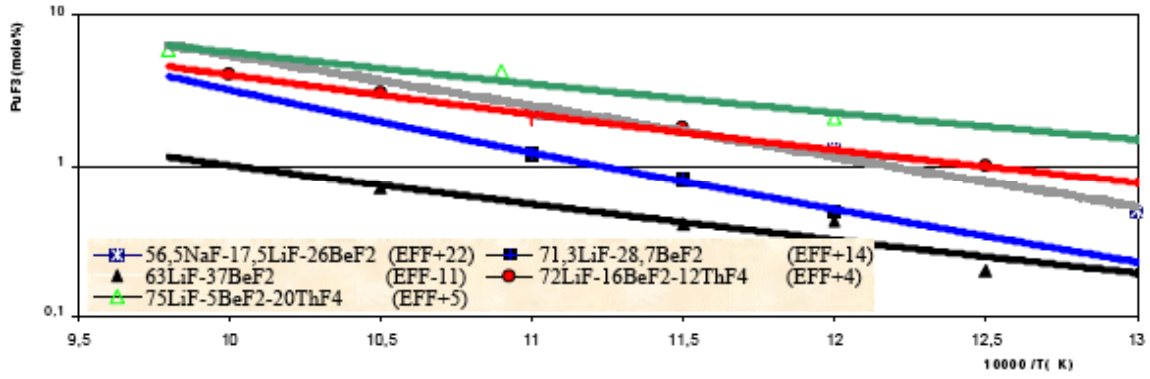

Figure 26. Solubility of PuF_3as a function of temperature in salt mixtures based on LiF-BeF_2 (Ignatiev et al., 2003).

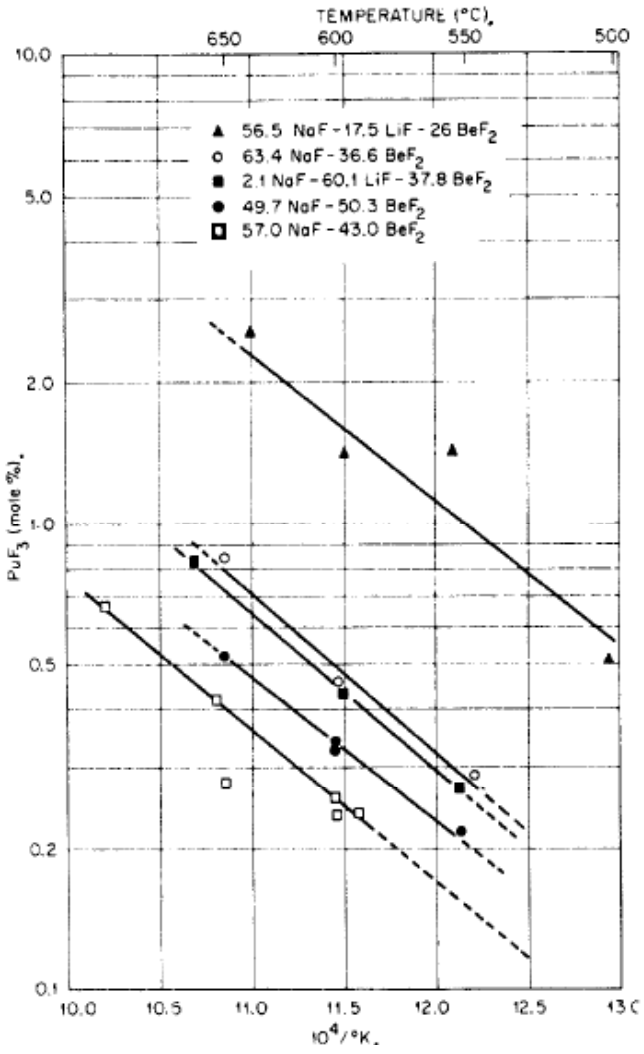

Figure 27. Solubility of PuF_3 as a function of temperature for $NaF\text{-}BeF_2$ and $NaF\text{-}LiF\text{-}BeF_2$. (Barton, 1960).

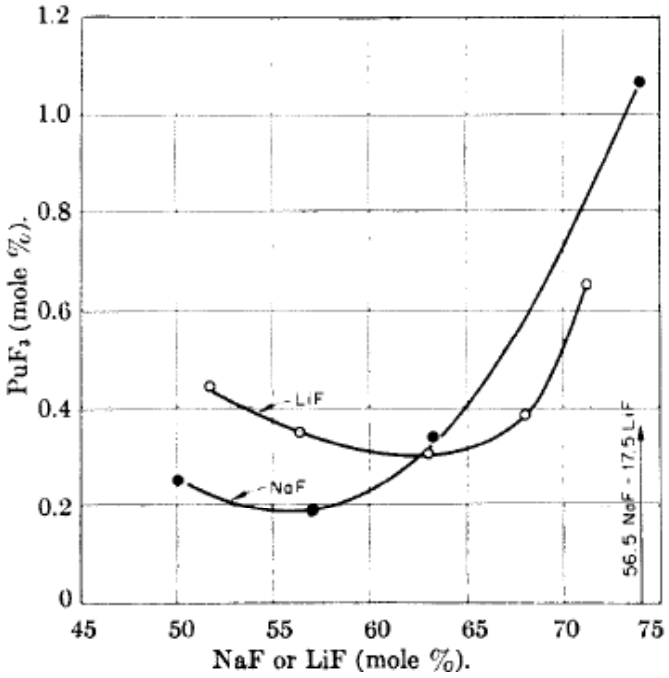

Figure 28. Solubility of PuF_3 (log of molar concentration) obtained with LiF-BeF_2 and NaF-BeF_2 salts versus 1/T (K). (Barton, 1960).

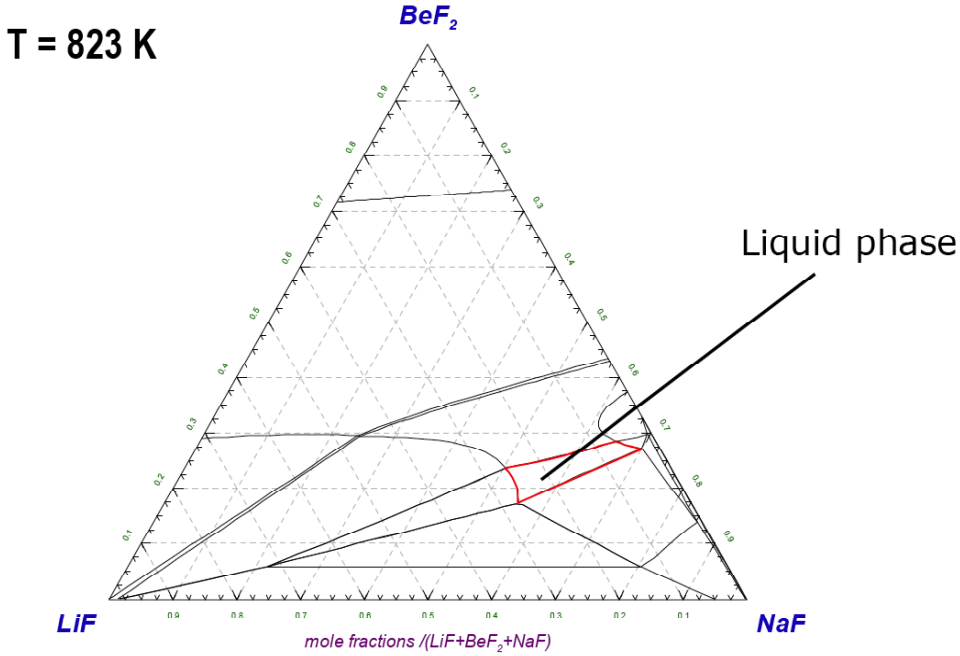

Figure 29. Isothermal section of the ternary LiF-NaF-BeF_2 phase diagram with fixed composition of PuF_3 (1.3 mole%), at 823 K (Benes and Konings, 2008).

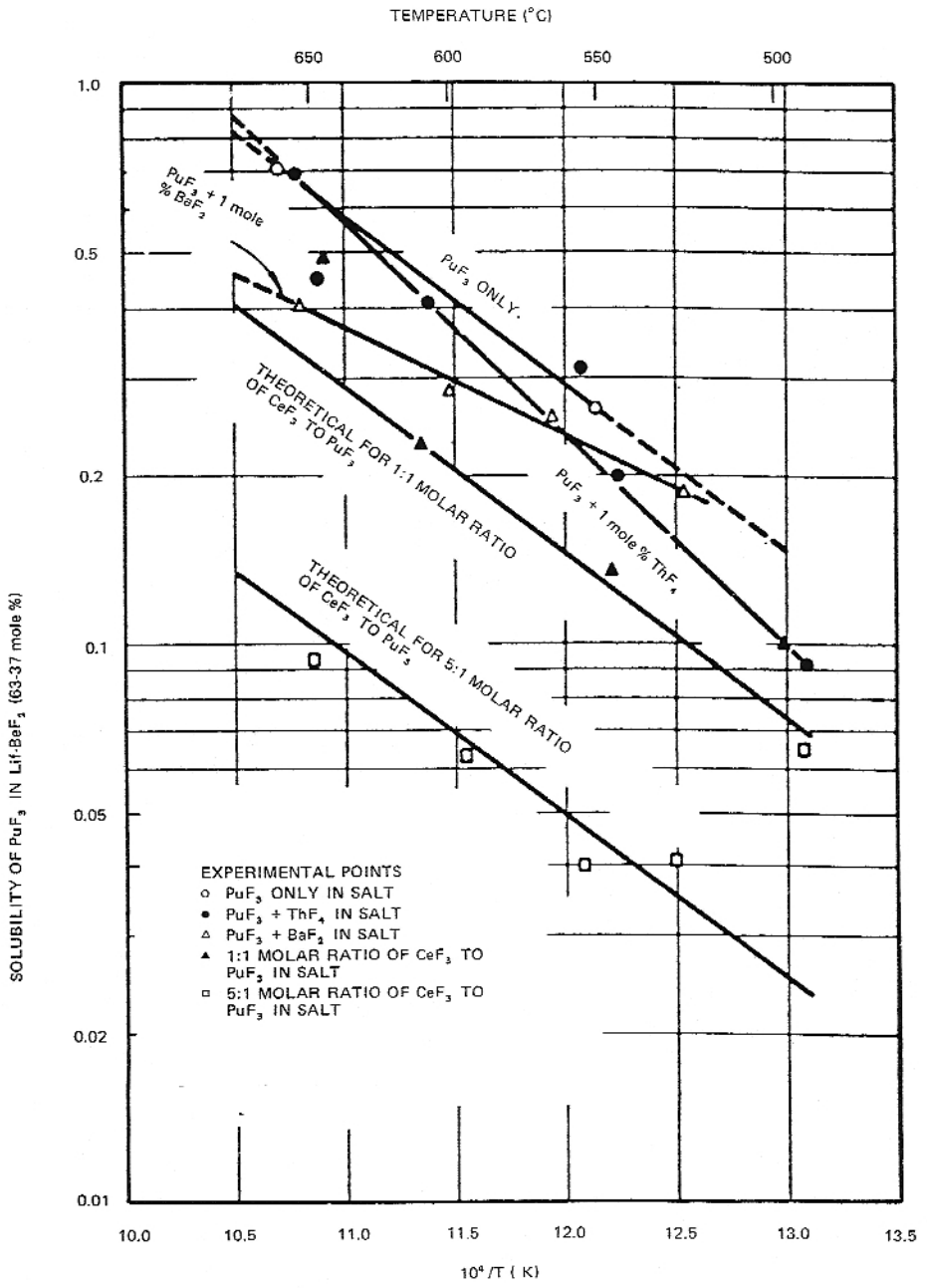

Fig. 12.8.2 Effect of Other Fluorides on Solubility of PuF_3 in $LiF-BeF_2$ (63-37 mole %) (59)(60)

Figure 30. Effect of CeF_3 on the solubility of PuF_3 in $63LiF-37BeF_2$ (mole%). (Barton, 1960).

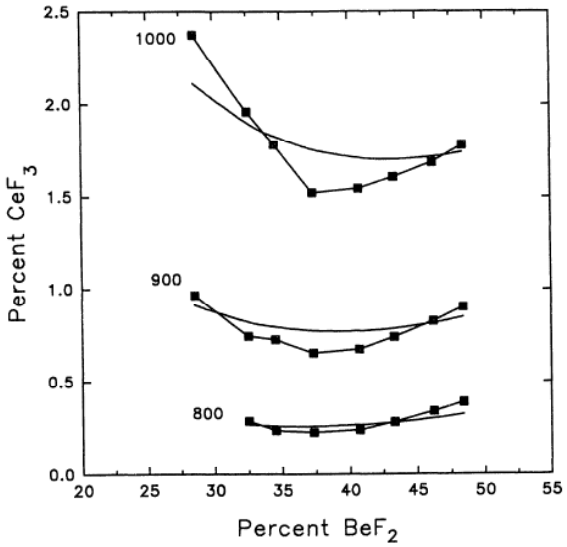

Fig. 5. Isothermal plots showing the solubility of CeF_3 in LiF-BeF_2 liquid. The lines are plotted from the calculations. The points are obtained by interpolation of the data using least square fits. See appendix.

Figure 31. Solubility of CeF_3 in liquid LiF-BeF_2 salt versus mole% of BeF_2 at 3 temperatures (Mulford, 1993).

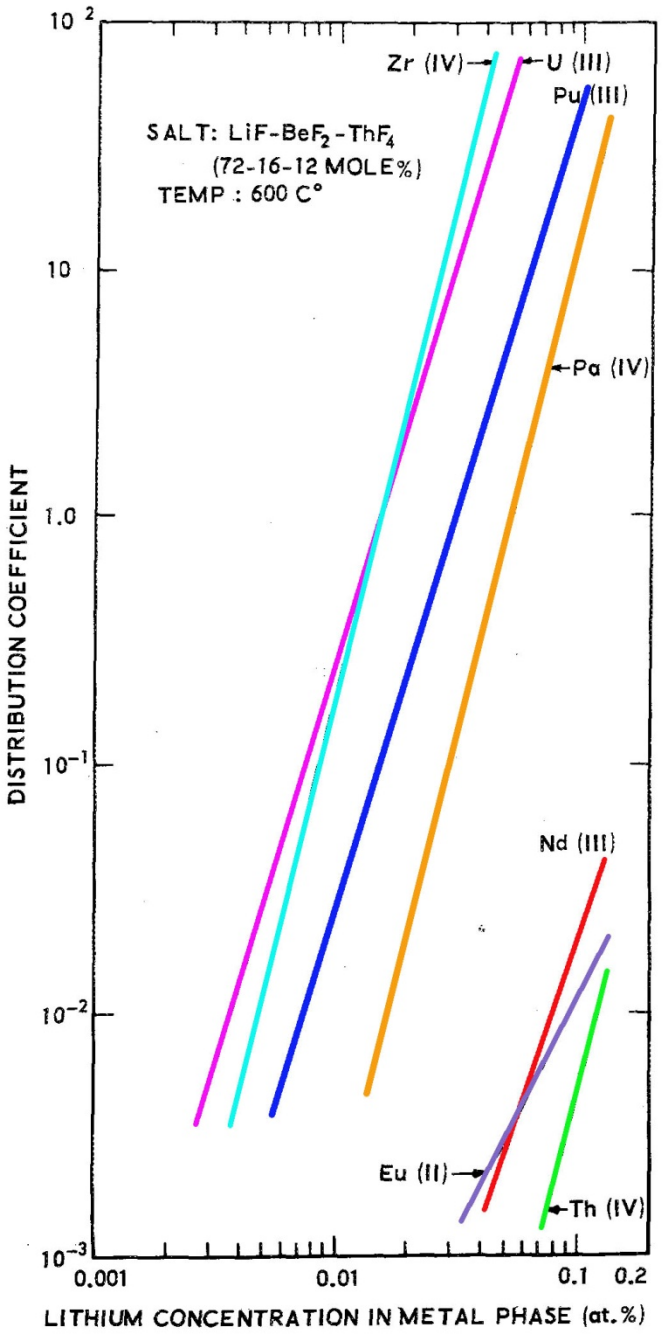

Figure 32. Distribution coefficients (concentration in metal/concentration in salt) of elements between molten Bi containing the indicated concentration of Li and molten LiF-BeF_2-ThF_4 salt at 600 ^oC (Whatley et al, 1970).

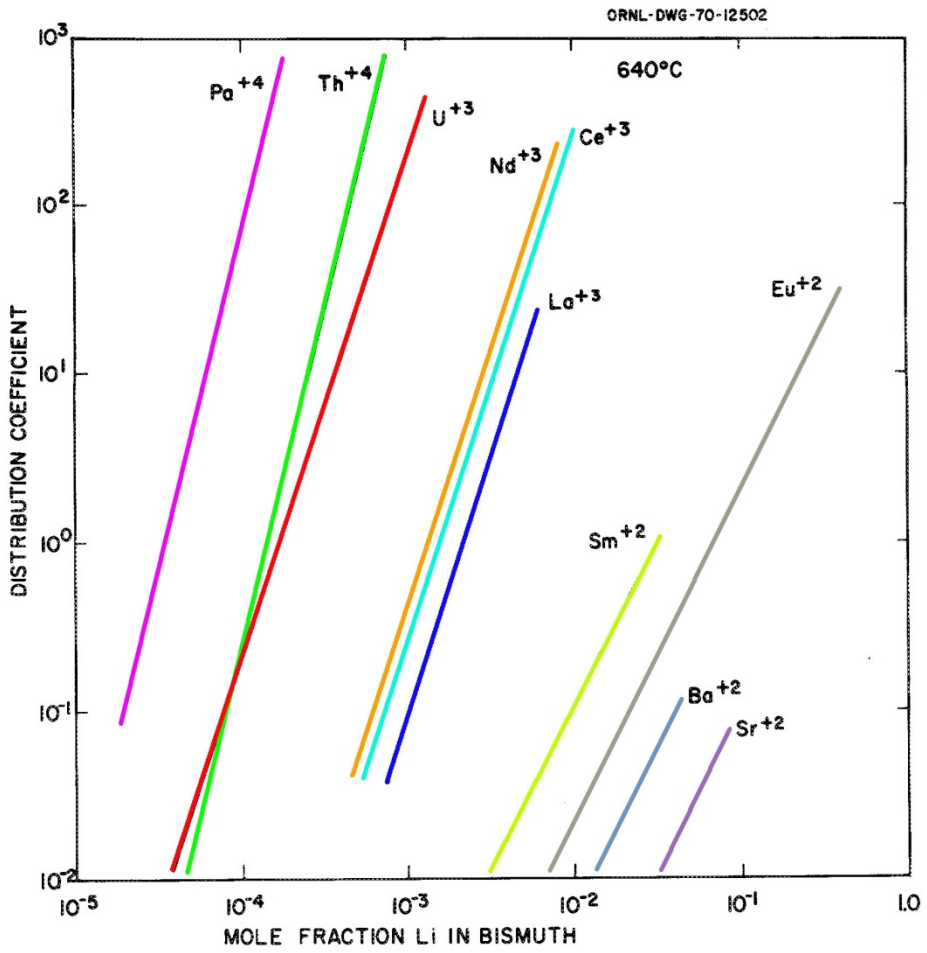

Figure 33. Distribution coefficients (concentration in metal/concentration in salt) of elements between molten LiCl and molten Bi containing the indicated concentration of Li at 640 ^{o}C (Rosenthal, Haubenreich and Briggs, 1972).

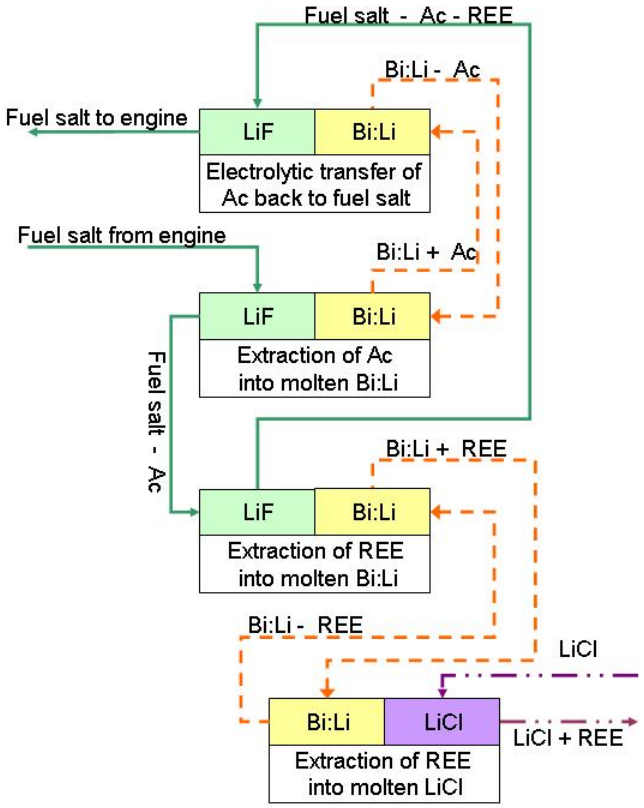

Figure 34. Conceptual scheme for the removal of REE from molten salt fuel. Cleanup of the LiCl containing the REE might be possible using an adaptation of ANL process for converting a chloride salt into a form acceptable for disposal in a repository.

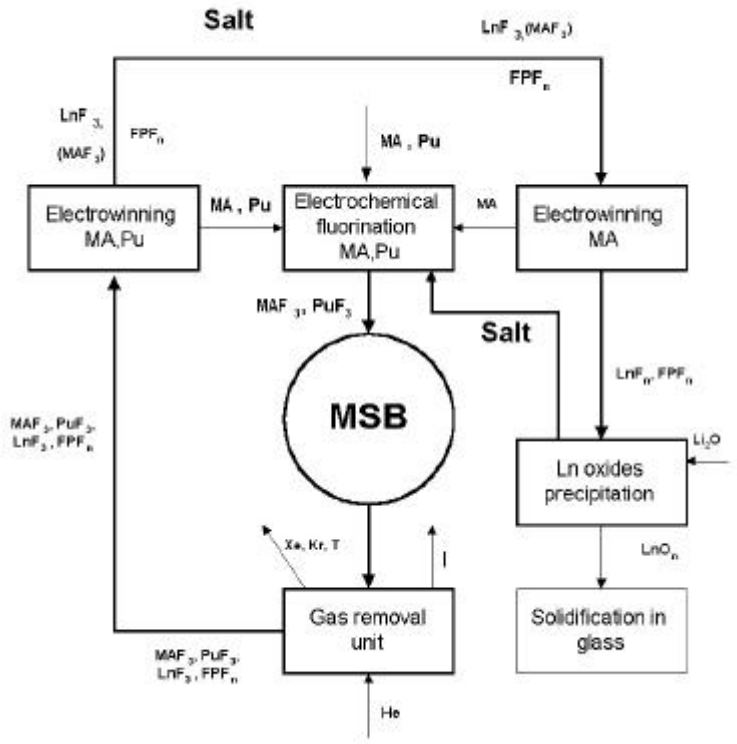

Figure 35. Conceptual scheme for the electrochemical separation of REE from molten salt fuel (Ignatiev, Gorbunov and Zakirov, 2004).

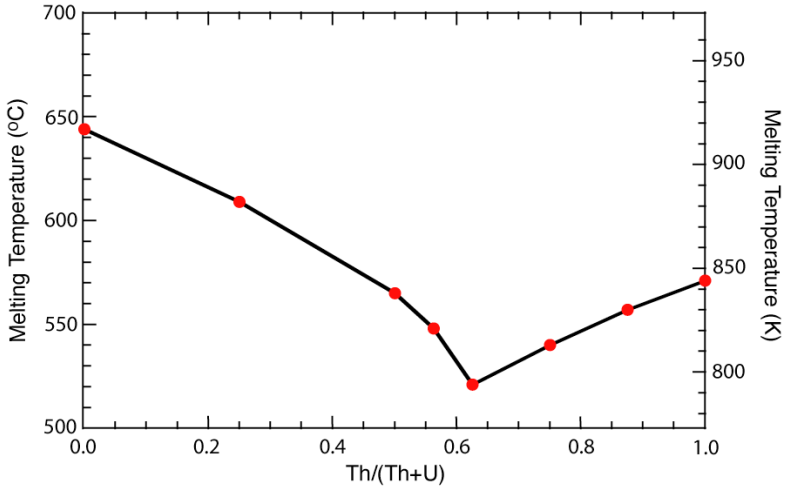

Figure 36. Melting temperature versus the ratio Th/(Th+U) for the molten salt compositions given in Table 8.